PRELIMINARY EXPERIMENTS ON THE CHARACTERISTICS AND POTENTIAL USES OF COAL FLY ASH FROM ISRAEL.

Henry A. Foner*, Thomas L. Robl, James Hower and Uschi M. Graham
University of Kentucky, Center for Applied Energy Research, 3572 Iron Works Pike, Lexington KY 40511

Keywords: Coal fly ash, Utilization, Israel

INTRODUCTION

Traditionally electric power in Israel has been produced from heavy fuel oil. Starting in 1982, the government-owned electric utility began to build coal-fired power stations and about 55% of the current output is now derived from coal. The switch to coal was made for strategic, economic and environmental reasons and future plans call for a continuing replacement of oil by coal for power generation.

Figure 1. Location of Power Stations

All power stations in Israel are on the Mediterranean coast (as shown in Figure 1) due to the need for copious supplies of cooling water which are unavailable elsewhere in the country. The coastal plain of Israel contains a large shallow aquifer which supplies a considerable part of the country's potable water. Most of the population is concentrated in this part of the country and this aquifer is already in considerable danger from anthropogenic pollution. Hence, there is much understandable concern about the effects of dumping large quantities of extraneous material anywhere on the coastal plain. It is for this reason that coal fly ash has been declared a hazardous waste material by the Israel Ministry of the Environment who put strict controls on its disposal. The only suitable site for dumping the ash is in the Negev desert south of Beersheva, and this entails considerable transportation costs. The practice of dumping the ash at sea at carefully chosen deep sites has now been stopped.

This paper surveys the present position and describes preliminary experiments on representative samples of coal fly ash. These experiments are intended to fully characterize the properties of the ash as a preliminary step to suggesting ways to utilize it as a useful material instead of treating it as an industrial waste.

ASH PRODUCTION AND DISPOSAL

The ash produced from the coal fired power stations has been disposed of as follows:

- Dumping in ash embankments at the Hadera power station.
- Use as an additive to cement by the Nesher Cement Co. (up to 10% allowed by the appropriate Israel Standard).
- A small amount as raw material for cement production.
- Dumping at sea (a limited amount under supervision of the Ministry of the Environment).

Table 1, reproduced from Metzger[1], summarizes the position - past and present.

TABLE 1

Amounts of ash produced, utilized and disposed of in Israel: Total and recent years (thousands of tonnes)

	1993	1994	1995	1982-95
Total Production	640	650	735	6060
Utilization/disposal:				
Cement production	420	440	630	3910
Embankments	150	160	20	1120
Disposal at sea	70	50	85	1030

* Permanent affiliation: Geological Survey of Israel, 30 Malkhei Yisrael St., Jerusalem 95501, Israel

Israel's electricity consumption is growing rapidly due to natural development and a rising standard of living and also because of the accelerated increase in population due to immigration. The current coal-fueled generating capacity is about 3,700 MW and this is scheduled to rise to 4,900 MW by the year 2000 with the addition of extra units to existing power stations. Total imports of coal for the year 1996 were about 7.5 million tonnes and of this all but 30,000 tonnes was used for electricity generation. As long term plans for electricity production are linked to coal, it is obvious that the amount of ash produced will increase and the problem of its disposal will become more acute. Ash production is expected to be 1,000,000 tonnes in 1997 and to reach 1,300,000 tonnes by the year 2001. In the year 2001 ash production will exceed the current level of utilization by approximately 700,000 tonnes. As the amount of ash used by the cement industry is near saturation, new uses must be developed, old uses expanded or the material must be exported if the undesirable prospect of ash disposal is to be avoided.

At present there are no flue gas desulfurization (FGD) plants on any of the coal fired power stations in Israel, so the potential problems of disposing of the by-products of such plants will not be considered here. However, FGD units will be erected in the Ashkelon power station by the year 2001 and subsequently may also be retrofitted in the Hadera power station.

EXPERIMENTAL and RESULTS

The Israel Ash Authority recently collected two carefully homogenized samples of fly ash for a study of the environmental effects of ash disposal and these were also used for the present study. These samples were chosen to represent the two main types of fly ash produced in Israel according to the type of coal burnt. The samples are designated as South African (SA) and Colombian (CO) after the (approximate) source of the parent coal.

Aqueous extracts of the fly ash samples are strongly alkaline (approximately pH 12 to 12.5) and the major chemical composition of the ashes is shown in Table 2[2].

TABLE 2

Analyses of reference samples of South African and Colombian Fly Ash

Element	**South African** %	**Colombian** %
SiO_2	44.0	56.5
Al_2O_3	33.2	23.5
TiO_2	1.8	1.2
Fe_2O_3	2.9	6.5
CaO	9.5	4.0
MgO	2.2	1.5
SO_3	0.8	0.6
P_2O_5	1.5	0.8

The samples were dry sieved into four fractions as shown in Table 3 and the carbon content of the fractions determined. The individual fractions were examined under both optical and scanning electron microscopes and the mineralogical properties of each fraction determined by X-ray diffractometry (XRD).

Table 3 shows the proportions of the various fractions present and the amount of carbon in each.

TABLE 3

Size fractions of the ash components and their carbon contents

Size		**South African**		**Colombian**	
Fraction	micron	%	carbon %	%	carbon %
>100 mesh	>150 μ	1.9	24.6	4.5	46.8
100-200	150-75	8.2	13.7	10.0	16.2
200-325	75-45	51.6	2.88	55.0	4.21
<325	<45	38.3	1.91	30.5	3.03

The original samples and the various fractions were examined under the optical microscope and the proportions of the following components determined: glass, mullite, spinel, quartz, isotropic coke, anisotropic coke and inertite. The predominant component (>90%) in both samples is glass. The total amount of carbon determined by this method for the original samples was 5.0% for SA and 7.4% for CO. These values compare with 4.2% and 7.1%, respectively, determined by a chemical method. Microscopic examination also shows that there is considerably more anisotropic coke (as defined by optical activity) present in the CO sample than in the SA sample.

Examination under the scanning electron microscope showed that the samples are typical fly ashes composed mainly of small aluminosilicate spheres. The carbon particles are relatively large and are porous with many glass spheres embedded in the interstices (Figure 2).

XRD spectra of the two samples showed some distinct differences. These were originally thought to be related to the presence of graphitic domain structures in the CO sample, but this aspect of the work needs further investigation. The graphitic character of anisotropic coke in fly ash has been commented on previously by Graham *et al.* [3]. The other minerals identified by XRD were: quartz, mullite and traces of lime.

DISCUSSION

The first step in any plan to encourage the use of fly ash as a raw material must be to supply a standard product with well defined properties. This product should conform to existing national or international standards. Perhaps the foremost of these is ASTM C 618 [4] which relates to the use of fly ash as a pozzolanic additive to Portland cement. This is an end use with a particularly high added value and Israeli ash is already used to some extent for this purpose. However, larger additions of fly ash to cement are quite common and, on the whole, improve the properties of the finished product. When the materials are examined on a size basis, distinct differences in the chemical and physical characteristics of the ash are found. These differences suggest that the separation of the ash into two fractions, a coarse +200 mesh (>75 μm) and a fine -200 mesh (<75 μm), would result in more usable products.

Carbon is preferentially fractionated to the larger sizes. The concentration of carbon found in the coarsest fraction of the material (+100 mesh or >150 μm) is probably sufficient to sustain combustion and may be recycled to the furnace to recapture its fuel value and increase overall fuel efficiency. The coarse fraction could also be further processed to concentrate the carbon for high value uses such as an adsorptive carbon as suggested by Graham *et al.*[3].

Carbon, however, is undesirable in fly ash used as a cement additive in concrete. It reacts with air entrainment reagents, is non-pozzolanic and may color the concrete if present in high enough concentrations. Because of these characteristics the loss on ignition (LOI), which for the most part is carbon, is limited by the ASTM C-618 standard to 6%. The fine fraction (-200 mesh or 75 μm) of both samples would easily meet this criterion. This may allow the proportion of fly ash currently used in cement in Israel to be increased beyond the current 10%. A substitution of 16% to 20% is typical for fly ash used in the U.S. The classification of the ash may also improve its pozzolanic properties. This would make it a more desirable material and encourage the development of an international export market.

The other suggested high volume use for fly ash is as a light-weight aggregate for building blocks. These could serve as a substitute for the no-fines concrete blocks which are now ubiquitously used, with the additional advantage of reducing the amount of quarrying and crushing needed for aggregate production.

Some other possible uses of fly ash are:

- as a light weight aggregate for aerated insulating building blocks.
- as a low strength flowable fill for trenches and around building foundations and basements.
- as the sand component of cement - Israel has a shortage of sand for concrete production in the densely populated parts of the country.

All these potential applications would be more profitable than using the fly ash as road-bed material and would be without the possible ecological disadvantages of this use.

REFERENCES

(1) Metzger, A.L. The Environmental Status of Coal Ash Produced in Israel. Proceedings of the 13th Annual International Pittsburgh Coal Conference, Pittsburgh, PA, September 3-7, 1996, 749-754.

(2) Cohen, H., Shepf, S., Dorfman, E. and Foner, H.A. Preparation of an Analytical Scheme for Coal Ash Leachates. Report to the Israel Ash Authority, May 1996.

(3) Graham, U.M., Robl, T.L., Rathbone, R.F. and McCormick, C.J. Adsorptive Properties of Fly Ash Carbon. Preprints of Papers presented at the 211th ACS National Meeting, New Orleans, LA, March 24-28, 1996, Vol. 41, No. 1, 1996, 265-269.

(4) Standard Specification for Fly Ash and Raw or Natural Pozzolan for use as a Mineral Admixture in Portland Cement Concrete. Annual Book of ASTM Standards, Vol. 4.02, ASTM, Philadelphia, PA, 11990.

ACKNOWLEDGMENTS

The authors wish to thank Dr. Samuel Grossman of the National Coal Supply Company, Israel, for his generous help with both the supply of samples and information. We also wish to thank our colleagues at CAER, Gerald Thomas and Margaret Grider, for carrying out analyses.

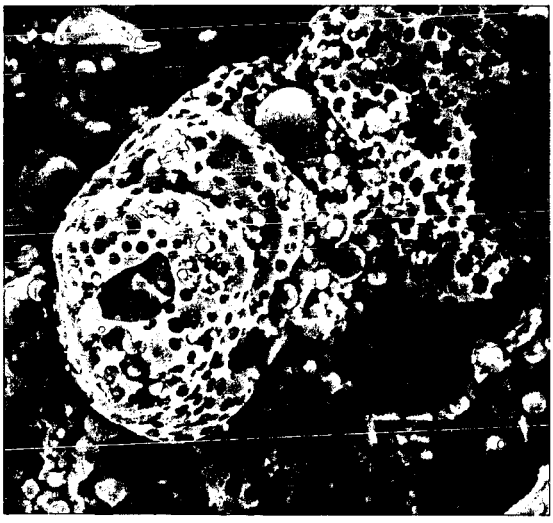

Figure 2. Porous carbon particle with embedded aluminosilicate spheres (Photomicrograph size approx. 80 x 80 μm)

STUDIES OF FLY ASH AND ASH DEPOSITS FROM AN AFBC SYSTEM

Wei Xie, Shi Su, H. Li, Wei-Ping Pan and John T. Riley
Materials Characterization Center and Department of Chemistry
Western Kentucky University
Bowling Green, KY, 42101

Keywords: combustion, fly ash, chlorine, sulfur

INTRODUCTION

The combustion of coal in a fluidized bed combustor with a limestone bed is one method of controlling sulfur oxides emission. Atmospheric Fluidized Bed Combustion (AFBC) results in two different kinds of solid residues, bed ash and fly ash. The formation of both bed ash and fly ash during the combustion of coal is a very complex environmentally dependent reaction. Significant parameters include the combustion conditions and the characteristics of the limestone used. If a high chlorine coal is used in an AFBC system, the addition of limestone may help reduce hydrogen chloride emission. On the other hand, due to the large amount of ash produced by a power plant, the use of these materials in an environmentally acceptable manner should be considered. The analysis of how the composition of the limestone changes during combustion can provide fundamental data, not only to evaluate the way the limestone functioned during combustion, but also to possibly determine how to use the residue.

During the last decade several studies have been conducted to characterize AFBC residues. Most of these activities focus on the physical properties of fly ash, such as particle size distribution, specific density, the morphological properties, and chemical properties which include the analysis of trace elements, organic compounds and chemical compositions. Knowledge of the distribution of elements such as sulfur and chlorine in fly ash is necessary, not only to understand the principle and efficiency of sulfation of limestone, but also to evaluate the role of the limestone in the capture of sulfur oxides.

EXPERIMENTAL

Experiments were conducted with the 12-inch (0.3 m) laboratory AFBC system at Western Kentucky University using operating conditions similar to those at the 160-MW system at the TVA Shawnee Steam Plant located near Paducah, KY. Two kinds of coal were used in this study, one is a low-chlorine (0.012% Cl and 3.0% S) western Kentucky # 9 coal (95011), the other is high-chlorine (0.28% Cl and 2.4% S) Illinois # 6 coal (95031). The limestone was from Kentucky Stone in Princeton, KY. Six moveable heat exchanger tubes are located within the bed area of the AFBC system. Typical operation involves setting the correct coal/limestone feeds and air flows and then using the moveable tubes to adjust the bed temperature to the desired setting. The combustor's operating parameters (air flow, coal/limestone feed, temperature) were adjusted according to the experimental requirements during combustion.

A TGA-501 thermogravimetric analyzer from the LECO Corporation in St. Joseph, MI was used for determination of the moisture and ash contents of the fly ashes. Carbon, hydrogen and nitrogen contents in the fly ashes were determined using a LECO CHN-1000 system. The sulfur contents were determined with a LECO SC-432 sulfur analyzer. Chloride contents were measured by bomb decomposition followed by determination of chloride with an ion selective electrode.

RESULTS AND DISCUSSION

Several parameters and their effects on the absorption of sulfur dioxide and HCl by the bed ash and fly ash were investigated. The parameters to be discussed in this paper include the bed temperature, the calcium-to-sulfur ratio in the combustion mixture, and the type of coal used.

The Effect of Bed Temperature on the Absorption of SO_2 and HCl. The sulfur contents of fly ash and bed ash reflect the different trends in ash composition that occur with changes in bed temperature. Figure 1 illustrates that the sulfur content in the fly ash increases as the bed temperature is increased. In contrast, Figure 2 shows that the sulfur content of the bed ash decreases with an increase in the bed temperature. At the lower temperature of 1116 K most of the sulfur dioxide produced during combustion is absorbed by the calcined limestone in the bed ash. The optimal sulfur retention is obtained around 1120K, where the sulfur retention reaches around 96%. With an increase in temperature, several factors may contribute to the reduction in the amount of SO_2 captured by the calcined limestone. At higher temperatures (>1120K) the active internal surface of the limestone particles is decreased, which may be due to the effect of sintering of limestone particles. At higher temperatures the equilibrium involving the formation of $CaSO_4$ from CaO, O_2, and SO_2 is shifted away from the formation of the sulfate salt and toward the free SO_2. As a result, more SO_2 is available to react with particles of lime in the fly ash and the sulfur concentration increases in the fly ash at the higher operating temperatures.

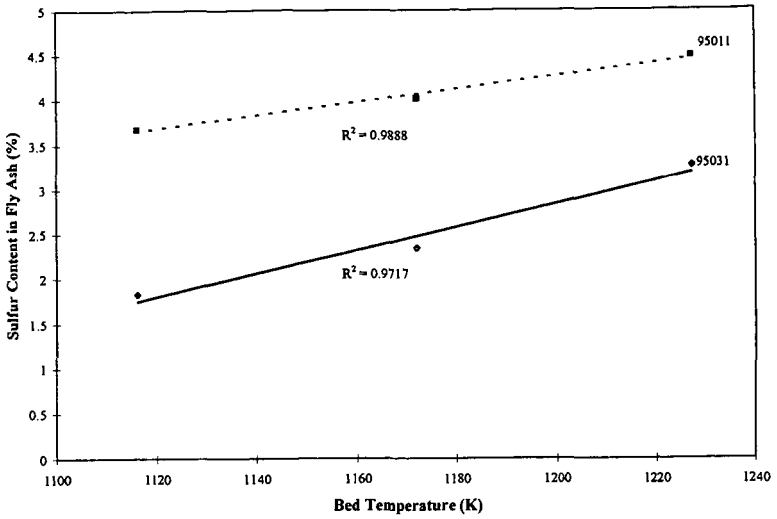

Figure 1. The effect of bed temperature on the concentration of sulfur in the fly ash of the AFBC system.

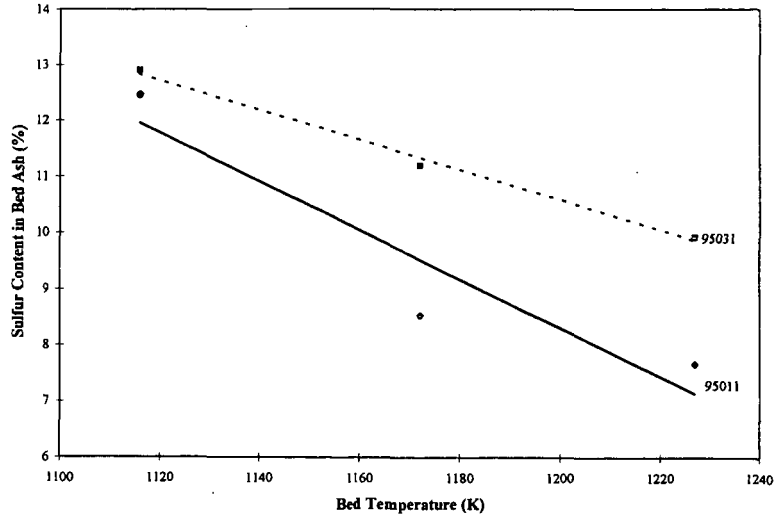

Figure 2. The effect of temperature on the concentration of sulfur in the bed ash of the AFBC system.

The effect of bed temperature on the chloride content in fly ash and bed ash are shown in Figures 3 and 4. It is obvious that the chloride content in the source coal is a decisive factor in the distribution of chloride in ash. The low chlorine coal (95011) released less hydrogen chloride during combustion and there are almost no temperature effects on the absorption of HCl in both the fly ash and bed ash from the combustion of this coal. For the high chlorine coal (95031), both Figures 3 and 4 show that chloride retention is more favorable at low temperatures.[1,2]

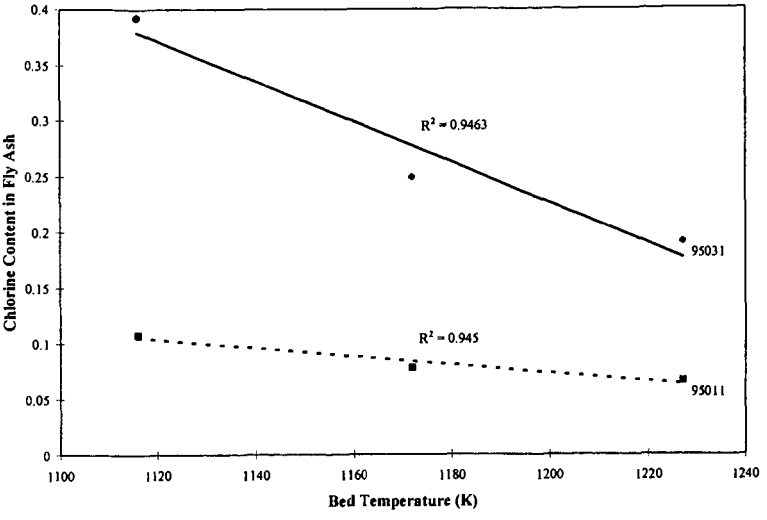

Figure 3. The effect of bed temperature on the chloride content in the fly ash from the AFBC system.

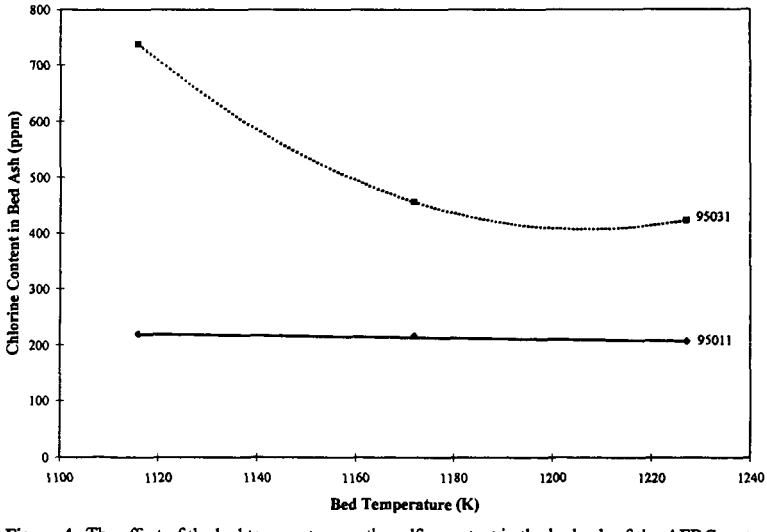

Figure 4. The effect of the bed temperature on the sulfur content in the bed ash of the AFBC system.

The Effect of Ca/S Ratio and Coal Type. Figures 5 and 6 show the effect of Ca/S ratio on the sulfur and chlorine retention in ash. One can see from these figures that the Ca/S ratio has more influence on the sulfur retention for the high sulfur content coal (95011). With the increase of the Ca/S ratio, the sulfur content in fly ash increased. Also, it can be seen that there is little effect of Ca/S on the chloride content in fly ash. On the other hand, Figure 6 shows that the Ca/S ratio is more important for the capture of chloride compared to sulfur for high chlorine content coal (95031). It is assumed that the HCl is probably captured in the low bed temperature region when the flue gas is passing through the heat exchange tube region because the reaction between HCl and CaO is more favorable at the low temperature.[1,2]

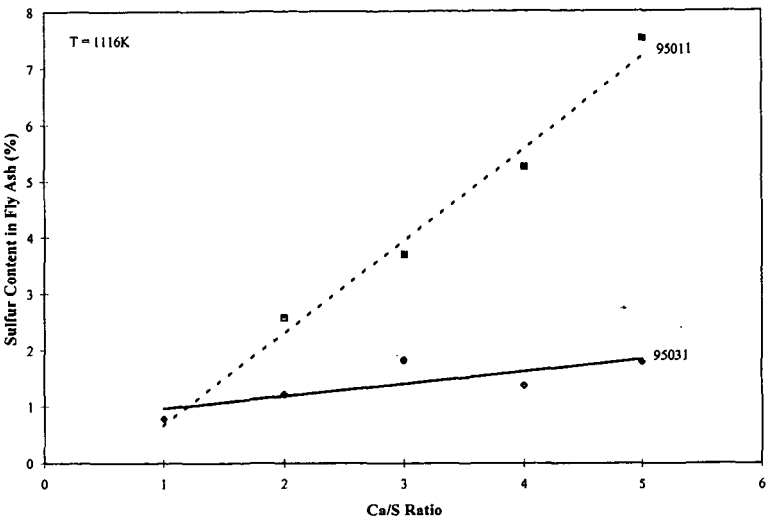

Figure 5. The effect of the Ca/S ratio on the sulfur content in the fly ash.

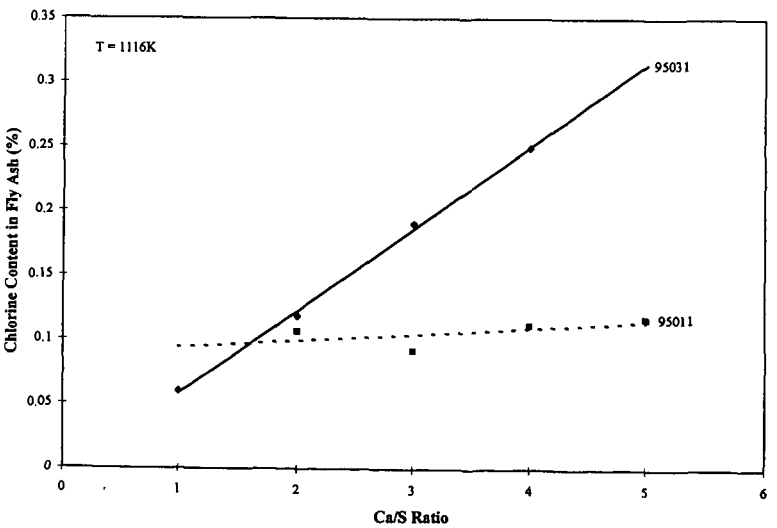

Figure 6. The effect of the Ca/S ratio on the chloride content in the fly ash.

CONCLUSIONS

Based on the data presented in this paper the following observations and statements can be made.

- The bed temperature in an AFBC system plays a key role in the retention of sulfur and chloride in ash. When the bed temperature is too high, less SO_2 is absorbed in the bed ash and more is absorbed in the fly ash.
- The chloride content of a coal is an important factor in the retention of chloride in the ash. Chloride retention in both the fly ash and bed ash is more favorable at low operating temperatures.
- When the sulfur or chlorine content in coal reaches a certain point, the Ca/S ratio in the combustion mixture will be an important factor in the absorption of SO_2 and HCl.

ACKNOWLEDGMENTS

The financial support for this work received from the Electric Power Research Institute is gratefully acknowledged.

REFERENCES

1. Bramer, E.A. "Flue gas emission from Fluidized Bed Combustion" in *Atmospheric Fluidized Bed Coal Combustion*," Elsevier, 1995.
2. Julien S.; Brereton, C.M.H.; Lim, C.J.; Grace, J. R.; Anthony, E.J. *Fuel*, **1996**, *75(4)*, 1655.

LONG TERM LYSIMETRIC LEACHING STUDIES OF FLUE GAS DESULFURISATION MATERIALS FROM THE COOLSIDE TECHNOLOGY.

Thomas L. Robl, Uschi M. Graham and Robert Rathbone, University of Kentucky, Center for Applied Energy Research, 3572 Iron Works Pike, Lexington, KY 40511, USA

Keywords

Flue Gas Desulfurization Material (FGD), Elemental Leaching, Mineralogic Transformations

Abstract

Flue gas desulfurization materials generated by a commercial test of the Coolside duct injection flue gas desulfurization technology was emplaced under controlled compaction conditions in a field lysimeter. Leachates were collected over a period of three years and the soil gases were monitored, as were the changes in the mineralogical and geotechnical properties of the materials. The dominant early reactions include the hydration of anhydrite ($CaSO_4$) to gypsum and the formation of ettringite ($Ca_6Al_2(SO_4)_3(OH)_{12}.26H_2O$). The dominant weathering reactions include the breakdown of gypsum and then ettringite through dissolution and carbonation reactions. The ultimate residual minerals being calcite and quartz. The original state of compaction was found to have a strong influence on the leachate chemistry with the highest compaction resulting in lower elemental concentrations and material wasteage. The leachates were composed primarily of Ca, Na, K and chloride and sulfate ions. The high pH's (10-12.5) favored the mobility of oxyanions.

Background and Methodology

This study was initiated during a successful test of the Coolside flue gas desulfurization technology at Ohio Edison's Edgewater generating station in 1991[1,2]. Coolside is a lime duct injection technology which is installed on the downstream side of the last heat exchanger. As tested by Ohio Edison, it also employs an alkali reagent, in this case NaOH, to enhance sulfur capture.

The overall goal of the this study was to develop sufficient chemical and physical data to insure the environmentally safe disposal of the material. The elemental release or leaching characteristics of the material was targeted for study.

Field studies included the controlled emplacement of the material under varying degrees of compaction in a field lysimeter (Figure 1). During the fill the geotechnical properties of the materials were measured. The lysimeters were excavated at the end of the project and the physical properties of the materials were again measured to determine the changes which had taken place.

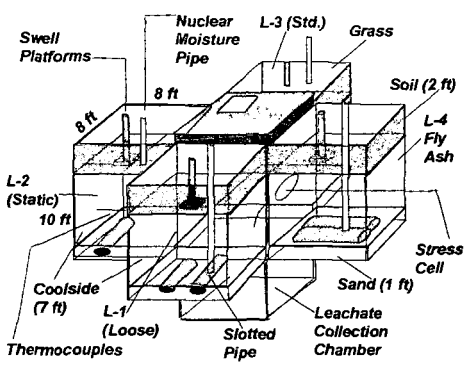

Figure 1. Diagram of Field Lysimeter.

The leaching properties of the material investigated included the determination of the chemistry of the leachate under laboratory column leaching and batch extraction (TCLP) conditions. The leachates from the field lysimeters were also collected and analyzed over a three and a half year period.

The physical and chemical properties of the materials are dependent upon complex mineral solution reactions. In an attempt to determine the overall controls on the system, detailed mineralogical determinations were made of the materials. Also, investigations were made into the state of the thermodynamic data available. A publicly available database and computer program was obtained from the United States Geological Survey and modified for this project[3].

Summary of Findings

Physical Properties of the Materials. Ninety-five percent (95%) of the Coolside material passed a 200 mesh sieve (-75 micron) and had a specific gravity of ~2.5. Index properties tests indicated that the Coolside materials were non-plastic and classified as ML (silt) in the Unified Classification System and A-4 under the ASSHTO System.

Table 1. Summary of chemistry from field leachates for first project year (March 1, 1993-February 28, 1994). Data in ppm except for pH and conductivity. Means not computed where more than 50% of samples were below detection limits.

	L1-3	N=44		L2-3	N=38		L3-4	N=52	
	Year 1	Year 1	Year 1	Year 1	Year 1	Year 1	Year 1	Year 1	Year 1
	Mean	Min	Max	Mean	Min	Max	Mean	Min	Max
Na	15767	5000	30000	15863	5300	33000	5480	3200	9100
Ca	800	335	1350	640	220	1340	45	18	90
K	5378	1640	8100	4764	1610	8000	1856	1000	3300
Al	ns	dl	dl	ns	dl	0.93	14.26	6.00	29.00
As	0.70	0.30	1.50	1.17	0.40	2.30	4.88	0.80	11.20
B	1.79	0.70	3.70	1.37	0.50	2.60	0.96	0.20	2.80
Ba	0.06	0.02	0.08	0.05	0.01	0.10	ns	dl	0.03
Cr	ns	dl	0.04	ns	dl	0.05	ns	dl	0.18
Fe	ns	dl	0.49	ns	dl	1.29	ns	dl	0.62
Mg	1.34	0.09	4.94	1.16	0.02	4.00	ns	dl	0.15
Mn	0.01	dl	0.04	ns	dl	0.05	0.03	dl	0.62
Mo	56.21	6.00	110.00	50.69	6.10	138.00	20.31	5.50	41.00
Se	2.44	0.30	3.70	1.85	0.25	3.55	1.09	0.24	2.00
Si	11.89	4.10	19.70	14.02	4.20	32.00	44.39	23.00	58.00
Ti	0.08	0.03	0.12	0.07	0.02	0.13	0.01	dl	0.02
V	0.54	0.28	0.98	0.85	0.07	1.80	1.56	0.92	3.47
Alk8.3	72	0	126	125	9	315	1905	275	4710
Alk4.5	186	139	314	249	143	550	3366	1573	7735
Cl	23908	1645	37590	23940	2380	46230	6897	2446	13200
Sulp.	17304	9000	20580	14311	2450	21410	2202	1214	3460
Br	nd	nd	nd	nd	nd	nd	1018	506	1960
pH	9.77	8.64	11.10	10.37	8.38	12.24	12.26	12.06	12.48
Cond.	70.18	19.40	102.00	66.21	19.80	108.30	28.56	14.90	48.50
D. Sol.	65677	16452	112500	59165	15772	107676	18462	8472	31122
S. Sol.	43	5	136	35	5	84	27	5	427

nd=not determined, ns=not significant, dl= below limits of detection

Table 2. Summary of chemistry from field leachates for third project year (March 1, 1995-March 29, 1996).

	L1-3	N=39		L2-3	N=26		L3-4	N=35	
	Year 3	Year 3	Year3	Year 3	Year 3	Year3	Year 3	Year 3	Year3
	Mean	Min	Max	Mean	Min	Max	Mean	Min	Max
Na	604	495	774	876	352	1635	1436	1035	2180
Ca	109	48	167	83	40	122	33	23	47
K	241	180	330	530	368	715	594	410	780
Al	0.47	0.20	0.92	1.11	0.45	1.74	12.69	10.50	16.20
As	0.30	0.21	0.44	0.47	0.15	0.77	1.16	0.85	1.60
B	0.57	0.30	0.85	0.68	0.30	0.95	0.21	0.05	0.48
Ba	0.01	0.01	0.02	0.02	0.01	0.03	0.01	0.01	0.02
Cr	0.01	0.01	0.03	ns	dl	dl	ns	dl	dl
Fe	ns	dl	0.28	ns	dl	0.20	ns	dl	0.12
Mg	ns	dl	0.10	0.06	dl	1.01	ns	dl	0.05
Mn	0.01	0.01	0.10	ns	dl	0.01	ns	dl	dl
Mo	0.93	0.52	2.00	1.36	0.61	2.90	3.40	1.75	5.00
Se	0.06	dl	0.11	0.09	dl	0.18	0.16	dl	0.45
Si	25.10	18.70	34.00	22.03	13.50	28.00	28.45	23.00	34.00
Ti	0.01	0.01	0.02	0.01	0.01	0.02	0.01	0.01	0.01
V	0.84	0.68	0.96	0.44	0.19	0.65	0.58	0.40	0.70
A8.3	129	0	262	144	66	258	563	288	920
A4.5	175	121	318	215	104	336	1033	799	1500
Cl	109	75	219	46	21	75	1408	838	2213
Sulp.	1506	1031	2052	2652	1671	5680	886	562	1510
Br	nd	nd	nd	nd	nd	nd	319	0	523
pH	11.15	10.95	11.34	11.32	10.91	11.54	12.00	11.84	12.19
Cond.	3.64	2.77	4.97	5.64	3.47	8.08	1.97	1.60	2.36
D. Sol.	2654	1850	3584	4276	2576	6870	5404	3872	7294
S. Sol.	5	5	10	5	5	5	6	5	25

Specimens compacted to 95% of maximum dry density (~1120 kg/m^3 or ~70 lbs/ft^3) and with optimum moisture (36.5%) were found to develop unconfined compressive strengths of between 1,000 psi and 2,500 psi (~6,900 to ~17,200 kPa). The compacted Coolside materials achieved permeabilities from 4 x 10^{-5} to 3 x 10^{-6} cm/sec (low to very low) in the lab.

Field Results. The field lysimeters were filled at three differing levels of compaction. Lysimeter L1 was loose filled (i.e. uncompacted) and had average dry density and moisture content of 706 kg/m^3 (44.1 lbs/ft^3) and 37.5%, respectively. Lysimeter L2 was compacted to the density designed to simulate the compactive efforts of a D9 bulldozer (117.3 kPa or ~17 psi). Dry density and moisture contents averaged 788 kg/m^3 (49.2 lbs/ft^3) and 38.9% in this lysimeter. The third lysimeter (L-3) was filled with Coolside material compacted near 95% of standard maximum dry density and optimum moisture content. Average values of dry density and moisture content were 1060 kg/m^3 (66.2 lbs/ft^3) and 37.0%, respectively.

After 3.5 years of weathering, the materials were excavated and their geotechnical properties determined. The average strengths of the materials in the three lysimeters were 44.1, 46.4 and 1,629 psi for the L1, L2 and L3 lysimeters respectively. Average permeabilities were 1.55 x 10^{-4}, 4.6 x10^{-4} and 2.2 x 10^{-6} for L1, L2, and L3 respectively. Thus, compaction had an overarching effect on the physical properties of the material. Achieving optimum compaction resulted in a fill which had substantial strength (layers of L3 achieved compressive strengths as high as 2,600 psi) and greatly reduced permeability (layers with permeabilities as low as 10^{-8} to 10^{-9} cm/sec were measured).

Mineralogy of the Materials The Coolside material as received was composed of quartz (SiO_2), mullite ($Al_6Si_2O_{13}$), portlandite ($Ca(OH)_2$)), calcite ($CaCO_3$), hannebachite ($CaSO_3$ $0.5H_2O$) and minor anhydrite($CaSO_4$). A glassy phase is also present in the raw Coolside material and typically consists of spherical Si-Al fly ash particles. Upon hydration ettringite ($Ca_6Al2(SO_4)_3$ OH_{12} 26 H_2O), the principal cementitious mineral in the system rapidly forms,

$$6Ca^{+2} + 2Al^{+3} + 3SO_4^{-2} + 12OH^- + 26H_2O = Ca_6Al_2(SO_4)_3OH_{12} \cdot 26H_2O$$

The state of compaction of the materials was found to have a strong impact on the chemistry of the leachates. Two distinct patterns emerged over the study. Lysimeters L1 and L2 initially had much higher elemental concentrations compared to L3 which was compacted to optimum density (Table 1). Sodium, Cl, K and sulfate were all higher in concentration by factors of 3 to 4 and Ca by a factor of more than 10 in L1 and L2 leachates. The longer term elemental release pattern showed a more rapid decline in elemental concentrations in the L1 and L2 leachates (Table 2). For example, Na in L1 dropped from an average value of 15,767 ppm--which is approaching the concentration of a brine--the first year, to an average value of 1,637 ppm the second year, and 604 ppm the third. The L3 leachates declined in concentration at a lower rate, with an average of 5,480 ppm the first year followed by averages of 2,302 ppm and 1,436 ppm the second and third year.

The leaching pattern for minor and trace elements did not necessarily show a similar pattern to that of the major elements. For example, Al and Si increased in concentration during the second year of the study in the L1 and L2 leachates as a function of pH of the leachates which increased over time.

The average pH of the L1, L2 and L3 leachates was 9.7, 10.4, and 12.3 during the first year of collection. Most transition metals are insoluble under these conditions and were not detected. However, elements which can form oxyanionic complexes such as Mo (MoO_4^{-2}), Se (SeO_4^{-2}), As (AsO_4^{-3}) and V (VO_4^{-3}) were found in measurable and sometimes significant concentration (e.g. Mo reached maximum concentrations >100 ppm in several samples the first year).

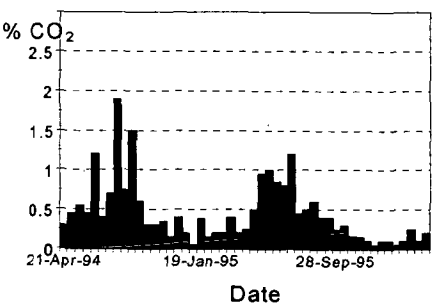

Figure 2. CO_2 Concentration in soil gas from 24 cm depth of lysimeter 1.

Carbon dioxide concentrations in the soil gases of the lysimeters were monitored in the second and third year of the study. In general, the highest CO_2 concentrations were reached during the summer and the lowest during mid-winter, as a function of respiration (Figure 2). The highest concentration recorded was 3.2% (32,000 ppm), well above that of atmospheric concentration (~350 ppm). Soil gas profiles gave clear and conclusive evidence of the highly reactive nature of the Coolside materials with respect to CO_2. At pH's above ~10 CO_2 reacts directly with hydroxide and forms carbonate ion,

$$CO_2 + 2OH^- = HCO_3^- = H^+ CO_3^{-2}$$

The thermodynamic analysis of the chemical composition of the leachates indicated that they are all supersaturated with respect to calcite and undersaturated with respect to gypsum and hannebachite. This, combined with direct mineralogical evidence, indicates that minerals are both dissolving and precipitating. The most important long term weather reactions include the precipitation of calcium carbonate and the dissolution of sulfites and sulfates, primarily hannebachite in this case, summarized as follows:

$$CaSO_3 1/2\ H_2O + 1/2O_2 + CO_3^{-2} = CaCO_3 + SO_4^{-2} + 1/2H_2O$$

Both the mineralogical and thermodynamic data indicate that ettringite will also break down over time. However this does not appear to proceed until the sulfate is largely exhausted. Thus, in effect, the sulfate acts as a buffer to extend the stability of the ettringite.

Elements of environmental concern which were found in concentrations exceeding RCRA limits included Se (RCRA limit 1 ppm) and As (RCRA limit 5 ppm). Some of the leachates from the L3 lysimeter reached concentrations as high as 19 ppm As during the first year of the study. The average concentration of Se for all of the leachates from the Coolside materials for the first year of study exceeded the 1 ppm limit.

References.

1. Ball, J.W., and D.K. Nordstrom, 99, WATEQ4F with Revised Thermodynamic Data Base and Test Cases for Calculating Speciation of Major, Trace, and Redox Elements in Natural Waters. USGS Open File Report 91-183.

2. Yoon, H., F.W. Theodore, F.P. Burke, B.J. Koch, 1986, Low Capital Cost, Retrofit SO_2 Control Technologies for High Sulfur Coal Applications. Reprint, Air Pollution Control Association, 79th Annual Meeting, Paper No. 86-47.5, 21 p.

3. Kanary, D.A., R.M. Statnick, H. Yoon, D.C. McCoy, J.A. Withum and G.A. Kudlac, 1990, Coolside Process Demonstration at the Ohio Edison Company Edgewater Plant Unit 4 - Boiler 13. *Proceedings, 1990 SO_2 Control Symposium*, EPRI and U.S. EPA, Session 7A, V 3, New Orleans, LA, 19p.

Acknowledgments

This work was funded by the United States Department of Energy, Contract No. DE-AC21-9MC2862 and the support of Peter Botros of that organization is gratefully acknowledged. We would like to thank our colleagues at the CAER Gerald Thomas, William Schram, William Atkins and Darrell Taulbee of the CAER and Tommy Hopkins and Tony Beckham of the University of Kentucky Transportation Research program for their help and support in this project.

A METHOD TO MEASURE BENZENE PRODUCTION DURING PYROLYSIS; RESULTS FROM TESTING OF CARBONACEOUS ADDITIVES IN FOUNDRY SANDS

Taulbee, D.N.[1], LaFay, V.[2], Dempsey, T.[2], and Neltner, S.[2]

[1]Univ. of Kentucky-Center for Applied Energy Research
3572 Iron Works Pike, Lexington, KY 40511
(606) 257-0238-ph, (606) 257-0302-fax

[2]Hill and Griffith Co.
1262 State Avenue, Cincinnati, OH

Keywords:benzene emissions, foundry, pyrolysis

ABSTRACT

Carbonaceous additives that are blended with clays in foundry sands and sand cores are recognized as a source of benzene emissions in the foundry industry. Impending legislation will possibly mandate substantial reductions in benzene emissions in this sector despite the fact that, with current technology, carbonaceous additives are essential for the production of quality castings. However, it may be possible to identify substitutes that provide acceptable casting performance while generating less benzene. As a first step, a method has been developed to measure the production of benzene during pyrolysis of carbonaceous materials. The method entails pyrolysis of carbonaceous samples in a thermogravimetric analyzer, absorption of the pyrolysis products onto activated charcoal, extraction of the charcoal with CS_2 containing p-cymene, and gas chromatographic quantitation of benzene. Results are presented for several potential sand-mold additives including a series of coals of varying rank, gilsonite, asphaltic suspensions, and metallurgical coke.

INTRODUCTION

It has been estimated that about 90% of all durable goods produced in the U.S. contain at least some metal castings.[1] During 1994, over 13 million metric tons of metal, ~85% of which were iron or steel, were processed by ~3,100 foundries in the U.S.[2] In 1996, the number of persons directly employed in the U.S. foundry industry numbered just over 220,000[3] which does not include the estimated hundreds of thousands of others that supply products to or sell finished goods from this sector. It is, therefore, clear that the foundry industry is a critical segment of the overall domestic economy, one that cannot be substantially curtailed without severe economic repercussions.

From 1971-1991, the domestic foundry industry declined by 32%, due in part to the implementation of increasingly stringent environmental protection regulations including the Clean Air Act (1970) and the Clean Air Act Amendments (1977 and 1990).[4] The most recent amendment calls for development and implementation of maximum achievable control technology (MACT) standards for the iron foundry categories by November, 2000. Meanwhile, some states are planning to implement their own regulations which set limits separate from those federally mandated. In Wisconsin, for example, sites that exceed such limits must either demonstrate emission controls that provide the lowest achievable emission rates (LAER) through technological advances or other options or show why they should be granted a variance.[5] In an effort to address the mandates of BACT and/or LAER, one of the options being examined by the foundry industry in that state is reformulation of the molding sand.

Though the carbonaceous materials added to sand molds and cores are believed partially responsible for unwanted emissions, they are essential in providing a reducing atmosphere during pouring which suppresses reaction between the casting sand and metal surfaces.[6] They also seal the voids between the sand grains thereby suppressing penetration of the molten metal into the sand mold.[7] The material most widely used to alleviate such casting defects is bituminous coal, commonly referred to in the foundry industry as seacoal. However, when subjected to high temperatures in a reducing atmosphere, i.e., pyrolysis, such coals generate one- and two-ring aromatics, both directly and via secondary reactions.[8] Of the aromatic components, benzene is of greatest concern due to its relatively high production and proven carcinogenicity. Numerous materials including petroleum resins, cellulosic flours, rosin and petroleum pitch, asphaltic emulsions, asphaltene chips, graphite, fuel oil, gilsonite, coal tar, and even sugar, starch, and molasses were developed as replacements for seacoal.[9] However, total displacement of seacoal by these additives was not realized for various reasons including uncertainties in availability and inferior performance. Today, the use of these replacements has either been discontinued or they are used as seacoal supplements, typically comprising 20-40 wt% of the carbonaceous additive. This latter trend of blending carbonaceous materials is believed to hold the most promise for reducing the release of hazardous pollutants. Accordingly, the work reported here represents an initial effort aimed at identifying potential additives that emit less benzene during casting yet meet the commercial criteria of low cost, acceptable performance, and availability.

EXPERIMENTAL

Briefly, measurement of the benzene-emitting potential entailed pyrolysis of carbonaceous additives by TGA, collection of evolved volatiles on activated charcoal, extraction of the charcoal with CS_2, and chromatographic quantitation of benzene. With the exception of the pyrolysis step, the method was modified from OSHA protocols for the measurement of benzene vapors in the workplace.[10]

Study Samples. A listing of the samples examined along with a brief description is given in Table I. All samples were solid materials with the exception of two proprietary aqueous asphaltic suspensions (AE-1 and AE-2). Several of these materials are currently used in commercially prepared green-sand blends including the bituminous coals, gilsonite, lignite, and the asphaltic emulsions. The solids were pulverized to the particle range as utilized in molding sands ranging from ~75% pass 40 mesh for the lignite to >90% pass 100 mesh for the gilsonite.

Pyrolysis. 20-90 mg samples were pyrolyzed in triplicate in a TA model 2950 thermo-gravimetric analyzer (TGA) under flowing Argon (60 mL/min). Following a 1 minute equilibration, the furnace was ramped from ambient to 800 °C at 100 °C/min and held for 5 minute. A fast heating rate was selected to more closely simulate the conditions within a sand mold during casting. The heating profile used for the aqueous emulsions was similar except that a 3-minute hold at 100 °C was substituted for the initial 1-minute hold. This modification was necessitated by the high water content of these samples which otherwise resulted in sample *splattering* from the pan. Weight loss from room temperature to ~200 °C was assigned to H_2O while losses above ~200 °C assigned to volatile matter.

Collection of volatiles. Glass tubes (~100 x 5 mm-i.d.) containing 20/40 mesh activated coconut charcoal (ORBO™-32) were used to collect the volatile matter generated during each TGA run. These tubes were partitioned into two in-series chambers; a primary containing 400 mg and secondary containing 200 mg of charcoal. The primary chamber, positioned nearest to the furnace exit, served to absorb the volatile matter as it evolved (including benzene) during the TGA run. The secondary chamber was used to ensure that benzene did not saturate and break through the primary. One end of the tube was loosely connected to the TGA-furnace exit while the other was connected to house vacuum. The vacuum was regulated such that roughly 200 cm^3/min gas flow was pulled through the tube. Thus, all carrier and pyrolysis gases exiting the TGA furnace were pulled into the charcoal tube without significantly affecting the furnace pressure.

Benzene quantitation. Prior to the extraction, benzene that is present in commercial-grade CS_2 was removed by passing the CS_2 through molecular sieve 13x, refluxing overnight with H_2SO_4/HNO_3 then again passing through molecular sieve. Chromatographic analysis of the processed CS_2 indicated complete removal of the benzene contaminants.

The charcoal from the primary chamber of each absorbent tube was transferred to a 4-mL, teflon-capped vial to which 2.00 mL of CS_2 spiked with *p*-cymene (10.24 ppm) was added. The vial was capped, shaken, and allowed to equilibrate at least 30 min at room temperature prior to analysis. Duplicate 1-2 μl injections of the extract were made into a HP5990 gas chromatograph equipped with a FID, a 10'x1/8" 20% SP2100/0.1% CW1500 column, and a HP-3390A integrator. Benzene was quantitated by comparison of the benzene/cymene ratios from the sample extract to a similar ratios from benzene/cymene standards, also prepared in CS_2. Due to interference with the cymene internal standard, benzene quantitation for gilsonite was achieved via an external standard technique.

RESULTS

Volatile Release Profile. TGA plots for the lignite, gilsonite, anthracite, and one of the bituminous coals (D4) are shown in Figure 1. Bituminous coal provides beneficial volatile matter release characteristics as evidenced by its common commercial usage in green-sand blends. The volatile release curve for gilsonite, also often used in commercial blends, is similar in that volatiles evolve over a relatively narrow temperature range, typically from 450-500 °C. This is in contrast to the weight loss curves for lignite and anthracite which are broader and occur at lower and/or higher temperatures. The weight loss curves for the asphaltic emulsions were reasonably similar to the D4 plot whereas weight loss for metallurgical coke was more similar to that from the anthracite.

It must be noted that the presence of carbonaceous materials in the sand mold is not of itself sufficient to assure good castings. Rather, it is the volatile component released during pyrolysis that plays the most significant role in creating a reducing atmosphere thereby minimizing oxidation.[11] Further, it has been shown that both the composition and temperature of release of the volatile matter governs the amount of *lustrous* or pyrolytic carbon formed (coke deposited onto the molten metal and adjacent sand).[12] Compelling evidence has also shown that only additives that are prone to lustrous carbon formation are of benefit in preventing burn-on.[13] Thus, the difference in volatile release profiles exhibited by the various materials in Figure 1 is likely an indicator of casting performance.

Method Reproducibility. Various aspects of the reproducibility of the method are shown by the data in Table II, obtained from replicate runs with the Birmingham seacoal. Columns 3 and 4 indicate the scatter in the moisture and volatile matter values from TGA was <5% rsd (σ-1) for this particular set of runs. Likewise, columns 6 and 7 indicate the range in peak integration reproducibility from duplicate injections was typically <10% relative to the mean. Finally, the last two columns indicate the overall reproducibility of the method was just over 1% rsd (σ-1) for this sample. This level of reproducibility was the best of the samples examined. However, the relative standard deviation was less than 5% rsd for most samples and less than 10% (Table III) for all samples with the exception of the anthracite and metallurgical coke from which benzene generation was very low.

Relative benzene generation. Benzene production, moisture content, and volatile matter release are shown for all samples in Table III. Benzene production ranged approximately two orders of magnitude from a low of <0.02 mg/g coal for the anthracite to approximately 2 mg/g for gilsonite. Benzene production is plotted versus volatile matter release in Figure 2. Not surprisingly, this plot shows that increased levels of volatile matter release results in a proportional increase in benzene generation. This implies that foundry-sand blends capable of generating the required levels of volatile matter during casting must obviously contain relatively greater quantities of those additives that generate less volatile matter (and less benzene) suggesting a near constant level of benzene production regardless of the additive. However, note that there are substantial differences in the ratio of benzene production to volatile matter release as shown in the last column of Table III. In general, those samples that generated less volatile matter during pyrolysis produced even less benzene on a relative basis. Thus, a 25 mg sample of lignite, for instance, would generate as much volatile matter on an absolute basis, as 10 mg of gilsonite while generating less than half as much benzene. The data in the final column of Figure 2 would, therefore, favor the use of anthracite, metallurgical coke, or lignite instead of bituminous coal or gilsonite in foundry sands. While this may well be true in terms of benzene generation, as discussed previously, suitable volatile release characteristics are critical for producing acceptable metal castings. In other words, it is not simply the quantity of volatile matter generated but the composition and temperature of release that are most important. In this respect, neither lignite nor metallurgical coke may be suitable as total replacements for bituminous coals (Figure 1) but may yet prove to be effective as partial replacements.

SUMMARY

A TGA pyrolysis/charcoal absorption method has been developed as a means to estimate the benzene-generating potential of carbonaccous additives in foundry sands. The method was shown to provide excellent reproducibility on samples ranging is size from 20 to 90 mg. Application of the method to a series of potential or currently used carbonaceous foundry-sand additives indicated substantial differences in the relative production of benzene during pyrolysis suggesting potentially fruitful areas for future work.

1. "Economic Analysis of Proposed Effluent Limitations and Standard for the Metal Molding and Casting (Foundry) Industry (Supplemental Analysis)"; Policy Planning & Evaluation, Inc.; Supplemental report submitted to the U.S. Environmental Protection Agency under Contract No. 68-01-6731; **1982**; 139 p.

2. "29th Census of World Casting Production-1994"; **1995**; Modern Casting; **85**; pp 24-25.

3. Employment and Earnings US Bureau of Labor, pub.; Washington, DC; March 1996.

4. Lassiter, M.J. "Foundries Prepare for Clean Air Act's Title V Showdown" **1994**, Editorial in Modern Casting, pp 58-59.

5. Personal communication with P. Kirsop, Plan Review Unit Supervisor, Compliance Section, Bureau of Air Management, Wisconsin Department of Natural Resources, Madison, WI.

6. Wang, C.; Heine, R.W.; Schumacher, J.S.; Green, R.A. "What's the Story on Seacoal Replacements in Foundry Sands?" **1961**, AFS Transactions, **73**, pp 496-503.

7. Lane, A.M.; Piwanka, T.S.; Stefanesev, D.M.; Giese, S.R. "Cast Iron Penetration in Sand Molds-Part I: Physics of Penetration Defects and Penetration Model" **1996**, *AFS Research Report*, CastExpo 96, April 1996.

8. Burnham, A.K.; and Happe, J.A. "On the Mechanism of Kerogen Pyrolysis" **1984**, Fuel, **63**, pp 1353-1356.

9. Dietert, H.W.; Doelman, R.L.; and Bennett, R.W.; "Mold Atmosphere Control"; **1944**; AFS Transactions; **52**; pp 1053-1077.

10. "OSHA Test Method No. 12 for Air Samples"; **1995** as taken from *Kentucky Occupational Safety and Health Standards for General Industry; 29 CFR Part 1910; 1910.1028 Benzene*; Promulgated by the Occupational Safety and Health Administration, U.S. Department of Labor; CCH Business Law Staff Pub., Chicago IL; 823 pp.

11. LaFay, V.S. and Neltner, S.L. "The Value of Seacoal and Seacoal Supplements in Today's Foundry Industry" **1987**, *AFS Transactions*, **95**, pp 133-137.

12. Bachmann, J. and Baier, D. "Some Aspects of Gas Evolution from Carbonaceous Materials Used in Foundry Molding Sands" **1974**, *AFS Transactions*, **82**, pp 465-471.

13. Stanbridge, R.P. "The Replacement of Seacoal in Iron Foundry Molding Sands" **1974**, *AFS Transactions*, **82**, pp 169-180.

ACKNOWLEDGEMENTS. The authors would like to thank Dr. J.C.Hower of the UK-CAER, for providing sample of anthracite.

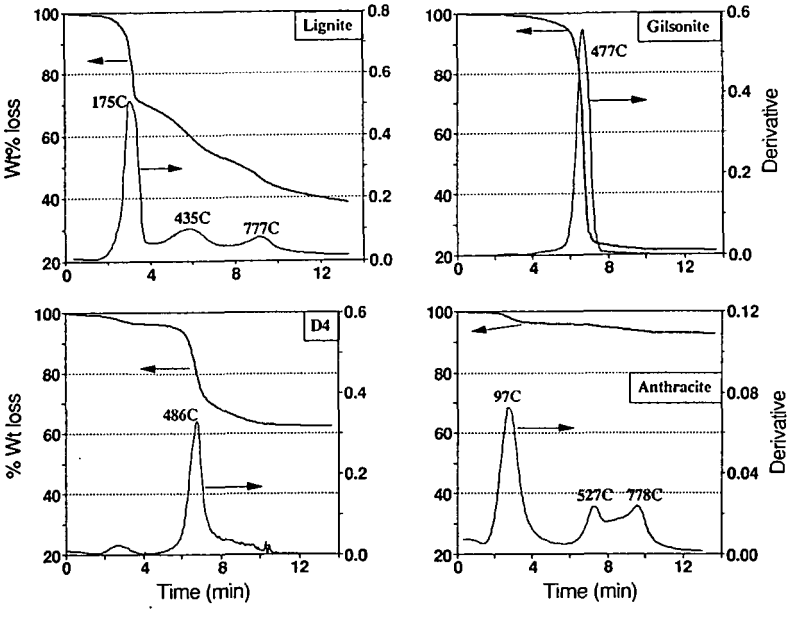

Figure 1. TGA plots showing weight loss and 1st derivative curves for lignite, Gilsonite, an asphaltic emulsion (AE-1), the D4 bituminous coal, and anthracite.

Table I. Listing and brief description of the samples examined.

Sample	Description
Anthracite	Mammoth coal bed, Schuylkill Co., PA
Met Coke	Commercial metallurgical coke
Lignite	Causticized lignite from North Dakota
Coal-Gran	Bituminous coal blended with 15% granulated sugar
D4 SC	Bituminous coal from West Virginia (washed)
Birm coal	Bituminous coal from West Virginia (washed)
Coal-liquid	Bituminous coal w/15% high fructose corn syrup
AE-1	asphaltic emulsion
AE-2	asphaltic emulsion
Gilsonite	gilsonite from Bonanze, Utah

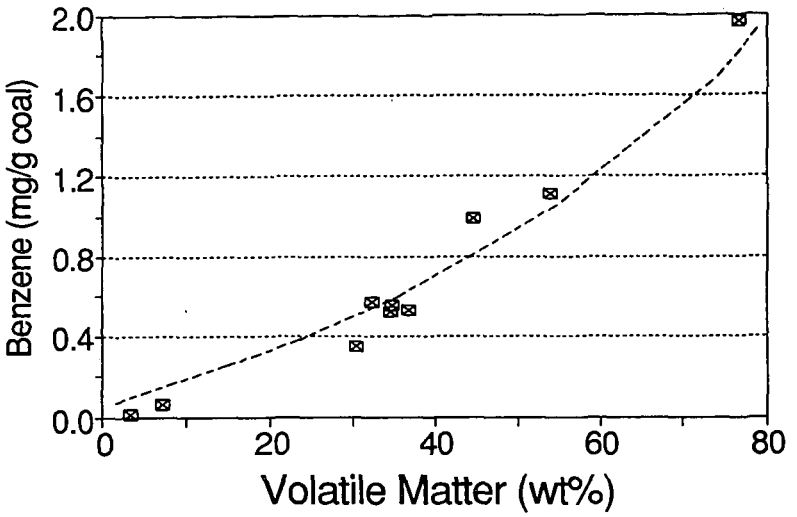

Figure 2. Benzene production as a function of volatile matter release during pyrolysis.

Table II. Method reproducibility as illustrated by replicate values from four TGA runs and duplicate GC injections (Birmingham coal sample).

TGA Run#	Sample Weight (mg)	Moisture by TGA (wt%)	Volatile matter (wt%)	GC Inj. #	Integrated Benz/cymene ratio	Total Benzene (ug)	Measured Benzene (mg/g coal)	Benzene Average (mg/g coal)
23	48.211	3.99	34.68	1st	1.408	26.26	0.545	0.549
				2nd	1.428	26.64	0.553	
24	42.883	3.90	35.46	1st	1.219	22.73	0.530	0.558
				2nd	1.349	25.16	0.587	
25	43.786	3.60	34.18	1st	1.302	24.29	0.555	0.553
				2nd	1.293	24.12	0.551	
26	34.140	3.73	34.47	1st	1.027	19.16	0.561	0.542
				2nd	0.958	17.86	0.523	
Mean		3.81	34.70				0.554	0.551
Std dev		0.151	0.475				0.016	0.007
rsd (%)		3.96	1.37				2.89	1.24

Table III. Benzene production (GC), moisture, and volatile matter (TGA) for all study samples.

Sample	# TGA runs	Moisture (wt%)	Vol matter (wt%)	Benzene (mg/g coal)	rsd (%) (sigma-1)	Benz/VM Ratio
Anthracite	4	3.88	3.45	0.019	22.5	0.006
Met Coke	4	0.92	7.32	0.065	35.2	0.009
Lignite	6	27.7	30.3	0.350	6.1	0.012
Coal-Gran	4	2.47	36.8	0.527	5.5	0.014
D4 SC	4	3.35	34.6	0.520	2.8	0.015
Birm coal	4	3.81	34.7	0.551	1.2	0.016
Coal-liquid	4	4.71	32.4	0.567	2.7	0.018
AE-1	5	35.8	53.9	1.117	6.9	0.021
AE-2	3	43.1	44.7	0.991	2.6	0.022
Gilsonite	3	0.88	76.6	1.972	2.9	0.026

IGNITION BEHAVIOR OF PULVERIZED COALS

John C. Chen,[†] Subrahmanyam Musti,[*] Vinayak Kabadi[*]
Departments of [†]Mechanical and [*]Chemical Engineering
North Carolina A&T State University
Greensboro, NC 27411

KEYWORDS: Coal ignition, coal reactivity, modeling

INTRODUCTION

We present data from a laser-based experiment used to measure the ignitability of pulverized coals in a room-temperature gas environment. The absence of hot furnace walls surrounding the test section allowed for optical detection of the ignition process. The experimental parameters studied include the coal type, oxygen concentration and particle size. The results show clearly that ignition reactivity is strongly dependent on coal type, and that the ignition rate constants determined are consistent with published data for overall combustion reactivity. The data also show convincingly that particle-to-particle variations in physical and/or chemical property of the fuel must be accounted for in order to model the ignition data correctly, and to accurately describe their ignition reactivity. We present a distributed activation energy model which accomplishes this goal.

EXPERIMENT

The experiment is similar to one described in detail elsewhere,[1] so only a brief description is given here. Figure 1 presents a schematic of the laser ignition experiment; the inset shows the details around the test section. Sieve-sized particles were dropped through a tube into a laminar, upward-flow wind tunnel with a quartz test section (5 cm square cross-section). The gas was not preheated. The gas flow rate was set so that the particles emerged from the feeder tube, fell approximately 5 cm, then turned and traveled upward out of the tunnel. This ensured that the particles were moving slowly downward at the ignition point, chosen to be 2 cm below the feeder-tube exit. A single pulse from a Nd:YAG laser was focused through the test section, then defocused after exiting the test section, and two addition prisms folded the beam back through the ignition point. Heating the particles from two sides in this manner achieved more spatial uniformity and allowed for higher energy input than a single laser pass. For nearly every case, two to five particles were contained in the volume formed by the two intersecting beams, as determined by previous observation with high-speed video.[2]

The laser operated at 10 Hz and emitted a nearly collimated beam (6 mm diameter) in the near-infrared (1.06 μm wavelength). The laser pulse duration was ~100 μs and the pulse energy was fixed at 830 mJ per pulse, with pulse-to-pulse energy fluctuations of less than 3%. The laser pulse energy delivered to the test section was varied by a polarizer placed outside of the laser head; variation from 150 to 750 mJ was achieved by rotating the polarizer. Increases in the laser pulse energy result in heating of the coal particles to higher temperatures. At the ignition point the beam diameter normal to its propagation direction was ~3 mm on each pass of the beam. An air-piston-driven laser gate (see Fig. 1) permitted the passage of a single pulse to the test section. The system allowed for control of the delay time between the firing of feeder and the passage of the laser pulse. Finally, ignition or nonignition was determined by examining the signal generated by a high-speed silicon photodiode connected to a digital oscilloscope, as described elsewhere.[1]

We report here the ignition behavior of two coals: one medium-volatile bituminous, and one high-volatile bituminous. Both samples were obtained from the Penn State University Coal Sample Bank, and the reported proximate and ultimate analyses are shown in Table 1. The coals were sieve-sized using a Ro-Tap shaker to -120/+140 mesh (106-125 μm diameter), and dried at 70°C under vacuum for at least 12 hours prior to each day's experiment.

RESULTS

Each day's experiment was conducted as follows: After choosing the coal and oxygen concentration to examine, the coal was loaded into the batch-wise feeder. The delay time between the triggering of the feeder and the appearance of the coal batch at the feeder tube exit was measured by visual observation in conjunction with a stop watch; typical values were ~2.9 s. The delay time was then programmed into the device which triggered the laser gate. The gas flow rate needed to achieve a drop distance of ~5 cm for the coal batch was also determined by visual observation. Finally, a laser pulse energy was chosen, and the experiment commenced. At each set of operating conditions (coal type and size, oxygen concentration, and laser energy), 20 attempts at ignition were made in order to measure the

ignition frequency, or probability, which is the parameter sought from these studies. Mapping this ignition frequency over a range of laser pulse energy produces an ignition-frequency distribution.

Such a frequency distribution is shown in Fig. 2 for the Pittsburgh #8 coal. It can be seen that at each oxygen concentration, ignition frequency increases monotonically over a range of increasing laser pulse energy. Below this range the ignition frequency is zero, and higher energies result in 100% ignition frequency. This behavior is due to the fact that, within any coal sample, there exists a variation of reactivity among the particles.[3] Thus, in this experiment, in which a batch of perhaps several hundred particles of a sample is dropped into the test section but only a few are heated by the laser pulse, there is an increasing probability (or frequency) as the laser energy is increased that at least one of the heated particles is reactive enough to ignite under the given conditions.

The repeated distributions under 100% oxygen, measured on separate days, show the excellent repeatability of this experiment; the most important factor for reproducibility is the moisture content of the sample.

Figure 2 also shows the effect of oxygen concentration: As oxygen level is decreased from 100% to 75%, and then to 50%, the frequency distribution shifts to higher laser energies or, equivalently, higher particles temperatures, as expected. This is consistent with ignition theory since at decreased oxygen levels, higher temperatures are necessary to achieve the equality between heat generation by the particles (due to chemical reactions) and heat loss from the particles. This equality is the minimum requirement for ignition, and is termed 'critical ignition.' The shift in distribution can be viewed in two ways: First, for a fixed laser pulse energy, a decrease in oxygen level leads to a decrease in the ignition frequency, all else being the same; second, a decrease in oxygen implies that a higher laser pulse energy is needed, in order to achieve the same ignition frequency.

Finally, it should be noted that for the Pittsburgh #8, the decreases in oxygen concentration shift the distributions to higher laser energies in approximately equal increments (equal energy ranges), and with little or no effect on the slope of the distributions. This finding is in contrast to the results for the Sewell coal (Fig. 3).

Three major differences between the ignition behaviors of the Pittsburgh #8 and Sewell exist. First, decreasing oxygen concentrations has a stronger effect in shifting the distributions of the Sewell to higher laser pulse energies (or higher particle temperatures). Second, as oxygen level is decreased, the slope of the distribution is undoubtedly decreased for the Sewell, while little effect is observed for the Pittsburgh #8. Finally, a comparison of the distributions of the two coals under 100% oxygen shows that the Sewell reaches 100% ignition frequency in a significantly smaller range of laser energy (ΔE_{laser} of ~150 mJ versus ~250 mJ).

DISCUSSION

Over the past three decades, many experiments have examined the ignition of pulverized coals under conditions which simulate pulverized fuel-firing conditions.[4,5,6,7,8,9] The common factor among these studies is the assumption of a single, average, kinetic rate-constant in describing the ignition reactivity of each coal. As we have shown previously,[3] it is necessary to account for the variation in reactivity among the particles within a sample in order to model the ignition distribution observed in this and nearly all previous ignition studies. Once such a model is implemented, the parameters may then be adjusted to fit the data and produce the desired ignition rate constant and reaction order with respect to oxygen for each coal.

Our previous experience in modeling ignition distribution data[3] provides some insight to explain the results described earlier. The model details will not be described here, but it is sufficient to note that the model accounts for particle-to-particle variations in reactivity by having a single preexponential factor and a Gaussian distribution of activation energies among the particles within a sample. The distribution is characterized by two parameters, an average activation energy (E_{av}) and a standard deviation (σ) in the activation energy.

In light of this model, the differences in the range of laser energies over which the various coals achieved 100% ignition frequency is a direct result of the breadth of the Gaussian distribution of activation energies: A narrow distribution (small standard deviation) leads to a small laser-energy range since most particles have similar activation energies and, thus, reactivities. Indeed, in the limit that the standard deviation is zero (all particles have the same activation energy), the ignition-frequency distribution would become a step function. Conversely, a broad distribution of reactivities (large σ) leads to a relatively larger range of

laser energy needed to achieve 100% frequency, as is the case for the Pittsburgh #8 compared to the Sewell. The effect of variations in the average value of the activation energy in the distribution is to shift the ignition-frequency plot; higher E_{av} means lower ignition reactivity for a particular coal, which would shift the ignition distribution to higher laser energies.

Finally, with regard to the effect of oxygen concentration on the slope and shift of the ignition-frequency distributions observed for the Pittsburgh #8 and Sewell coals, the model interprets such differences to be the result of the variation in the reaction order, n, with respect to oxygen concentration.

The model results for the Pittsburgh #8 coal are shown in Figs. 4, 5 and 6, for average particle sizes of 115 μm, 69 μm and 165 μm, respectively. The model parameters (E_{av}, σ, and n) were adjusted to produce the best fit at all oxygen concentrations for the 115 μm particles (Fig. 4). They were then left at these values to produce the results for other particle sizes (Figs. 5 and 6).

As can be seen, while the model captures salient features in the experimental data, the fit to the data is not ideal. This is attributed to a lack of knowledge of the particle temperature at ignition. Indeed the results shown relied on calculated temperatures as described previously.[1] We plan to improve the experiment by implementing a two-color pyrometry system to directly measure the ignition temperature in future studies.

ACKNOWLEDGEMENT

The support of this project by the U.S. Department of Energy through Grant DE-FG22-94MT94012 is gratefully acknowledged.

REFERENCES

1 Chen, J.C., Taniguchi, M., Narato, K., and Ito, K. "Laser Ignition of Pulverized Coal," *Combust. Flame* 97, 107 (1994).

2 Chen, J.C., Taniguchi, M., Ito, K. "Observation of Laser Ignition and Combustion of Pulverized Coals," *Fuel*, 74(3), 323 (1995).

3 Chen, J. C. "Distributed Activation Energy Model of Heterogeneous Coal Ignition," *Combust. Flame*, 107, 291 (1996).

4 Essenhigh, R.H., Mahendra, K.M., and Shaw, D.W. *Combust. Flame*, 77, 3 (1989).

5 Cassel, H.M. and Liebman, I. *Combust. Flame*, 3, 467 (1959).

6 Karcz, H., Kordylewski, W., and Rybak, W. *Fuel*, 59, 799 (1980).

7 Fu, W. and Zeng, T. *Combust. Flame*, 88, 413 (1992).

8 Zhang, D., Wall, T.F., Harrie, D.J., Smith, I.W., Chen, J., and Stanmore, B.R. *Fuel*, 71, 1239 (1992).

9 Boukara, R., Gadiou, R., Gilot, P., Delfosse, L., and Prado, G. *Twenty-Fourth Symposium (International) on Combustion*, The Combustion Institute, Pittsburgh, PA, 1993, pp. 1127-1133.

Coal		Prox. Analy. (dry wt%)		Ultimate Analysis (dry, ash-free wt%)				
Penn State ID	Rank	Vol. Matter	Ash	C	H	N	S	O (diff.)
Pittsburgh #8 (DECS 23)	low-volatile A bituminous	39.4	9.44	82.0	5.63	1.49	4.27	6.66
Sewell (DECS 13)	medium-volatile bituminous	25.0	4.22	88.2	4.95	1.50	0.65	4.71

Table 1: Ultimate and proximate analyses of coals used in this study.

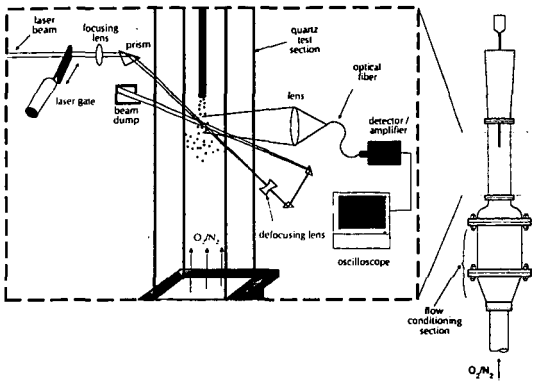

Fig. 1: Schematic of the laser ignition experiment.

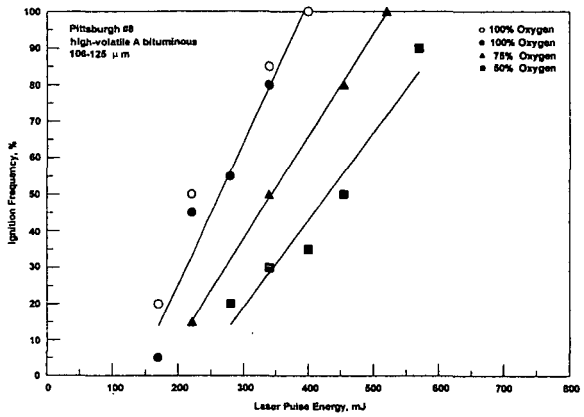

Fig. 2: Ignition-frequency distributions for the Pittsburgh #8 coal. Two data sets (open and filled circles) at 100% oxygen show reproducibility of experiment. Solid lines represent linear regressions of each data set.

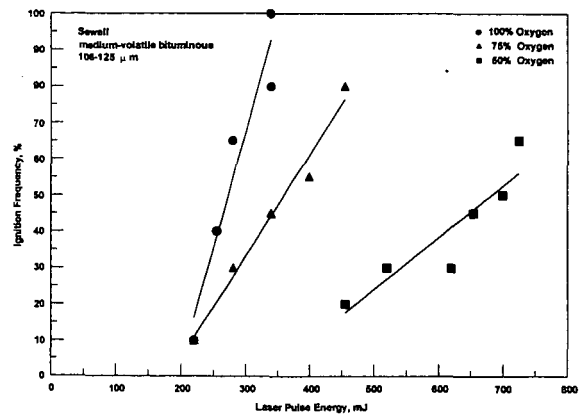

Fig. 3: Ignition-frequency distributions for the Sewell coal. Solid lines represent linear regressions of each data set.

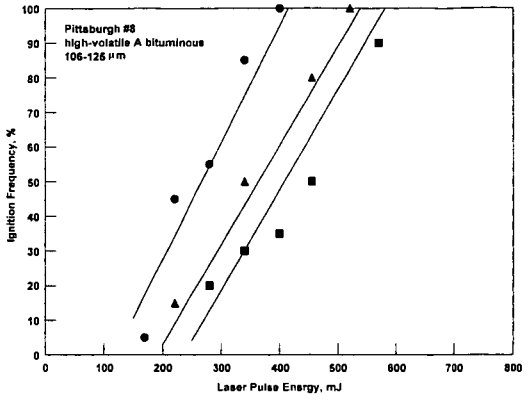

Fig. 4: Comparison of experimental data to model for 115 μm particles. Lines represent linear regressions of experimental data and symbols are from simulation.

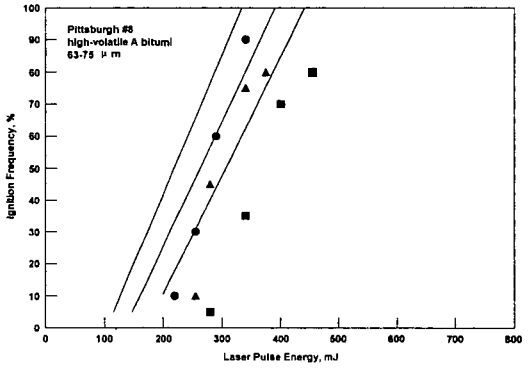

Fig. 5: Comparison of experimental data to model for 69 μm particles. Lines represent linear regressions of experimental data and symbols are from simulation.

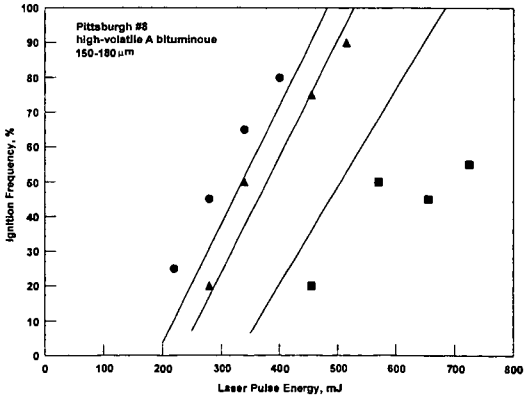

Fig. 6: Comparison of experimental data to model for 165 μm particles. Lines represent linear regressions of experimental data and symbols are from simulation.

STUDIES OF CHLORINE AND SULFUR BEHAVIOR DURING COAL COMBUSTION IN AN AFBC SYSTEM

Wei Xie, Wei-Lan Pan, David Shen, Wei-Ping Pan and John T. Riley
Materials Characterization Center and Department of Chemistry
Western Kentucky University
Bowling Green, KY 42101.

Keywords: combustion, sulfur, and chlorine

INTRODUCTION

The laboratory sized atmospheric bed combustor (AFBC) at Western Kentucky University was designed to serve as a flexible research and development facility to gain operating experience, evaluate combustion performance, and estimate the effects of flue gas emissions. The operating conditions for the AFBC system are similar to those used at the TVA 160-MW AFBC Pilot Plant located near Paducah, Kentucky. Fluidized bed combustion systems are particularly suited to waste fuels because of their ability to burn low grade and variable fuels as well as absorb sulfur oxides through the use of limestone.

It has been demonstrated that the following parameters have an effect on the amount of sulfur retained in the fluidized bed: the molar calcium-to-sulfur ratio, the sorbent particle size, the gas phase residence time, sorbent reactivity, bed temperature, feed mechanisms, and excess air level.[1] The amount of limestone sorbent needed in a fluidized-bed combustor is proportional to the sulfur contained in the fuel and inversely proportional to the amount of calcium contained in the limestone. Calcium in the limestone which can be reacted with sulfur oxides depends on factors specific to the limestone and to the operating conditions in the fluidized-bed combustor.

The chloride content of coal varies from just a few ppm to thousands of ppm. Emissions of chloride from coal-fired plants can range from 50 to several thousand parts per million by volume, depending on the original concentration in the coal, the type of combustor, and any pollution control equipment installed. It has been estimated that 94% of the chloride in coal is volatilized, generally being emitted as gaseous HCl.[2] In an AFBC system limestone may be able to capture the chlorine. Limestone degenerates to CaO, and CaO reacts with HCl to produce $CaCl_2$.[3] In an AFBC system, capture of chloride by limestone in the combustion zone depends upon the temperature of the combustion zone and the ratio of calcium-to-sulfur. A study by Liang and others[4] showed that chloride capture has a large variation with temperature moving from a low of 18% gaseous HCl at 700°C to 99% HCl at 950°C. The resulting product is almost entirely in the form of liquid $CaCl_2$. Munzner and Schilling[5] studied the effect of limestone in a bench-scale AFBC system. The results showed that a greater recapture of chloride occurred with larger excesses of limestone, or when the Ca/S ratio was greater than 2.

To better understand the combustion behavior of sulfur and chlorine during coal combustion in an AFBC system, a comprehensive research project was performed at the Western Kentucky University on different aspects of emission reduction from fluidized beds during coal combustion. Some results of this study are reported in this paper.

EXPERIMENTAL

Two 1,000-hour burns were conducted with the 12-inch laboratory AFBC system at Western Kentucky University. Operating conditions similar to those at the 160-MW system at the TVA Shawnee Steam Plant located near Paducah, KY were used. A 1,000-hour burn was done with a low-chlorine (0.012% Cl and 3.0% S) western Kentucky # 9 coal (95011), which is the same type of coal as that supplied to the TVA plant during 1993. A second 1000-hour burn was conducted with high-chlorine (0.28% Cl and 2.4% S) Illinois # 6 coal (95031). Six moveable heat exchanger tubes are located within the bed area. Typical operation involves setting the correct coal/lime feeds and air flows and then using the moveable tubes to adjust the bed temperature to the desired setting. The combustor's operating parameters (air/water flow, coal/lime feed, bunker weight, temperatures and pressures) were controlled and logged to file with a Zenith 150 MHZ PC utilizing the LABTECH software version 3.0. During the combustion runs any needed changes in the parameters could easily be entered into the computer by accessing the correct control screen and making the necessary corrections on line. During combustion runs the flue gases at the heat exchanger region were analyzed continuously using on-line FTIR, GC, and IC instrumentation.

RESULTS AND DISCUSSION

The major operating parameters for the AFBC system were as follows: excess air level -- approximately 1.3; Ca/S ratio -- approximately 3; bed temperature -- 1144K, CO_2 level -- approximately -- 13%; oxygen in the flue gas -- 5-6%. Figure 1 shows the O_2 and CO_2 concentrations

in the flue gas at various positions above the fuel injection port. The influence of different process parameters on the emissions of SO_2 and HCl will be discussed.

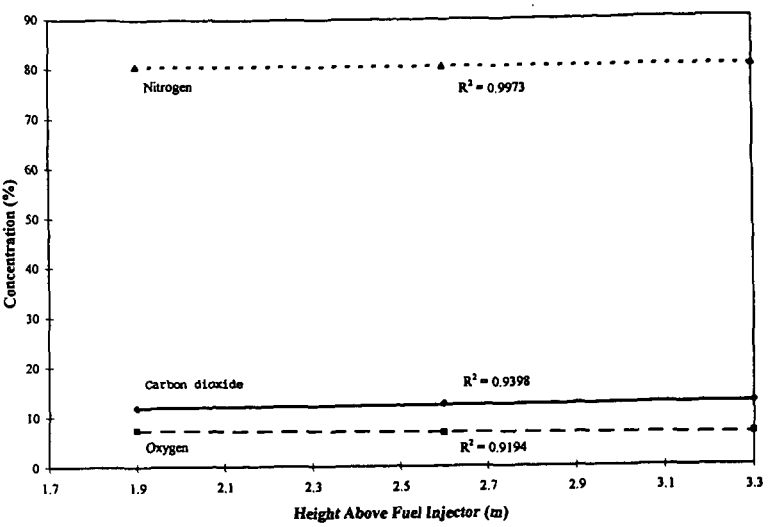

Figure 1. Flue gas composition in the center of the AFBC combustor at different heights above the fuel injection port.

The Effect of Bed Temperature. Figure 2 shows that the SO_2 emission increases as the bed temperature is increased. The optimal sulfur retention is obtained around 1120K. The sulfur retention reaches around 96% at this temperature. At higher temperatures (>1120K), the active internal surface of the limestone particles is decreased, which may be due to the effect of sintering of limestone particles. The thermal decomposition of the $CaSO_4$ under reducing conditions (such as in the presence of CO, hydrogen, or carbon) at the higher temperature may also contribute to the emission of SO_2. The effect of temperature on the emission of chloride is shown on the Figure 3. More HCl is observed when the temperature was raised to the higher temperature. The capture of HCl by limestone is more difficult than the capture of SO_2. Also, the reaction between HCl and CaO is more favorable at the lower temperature.[4]

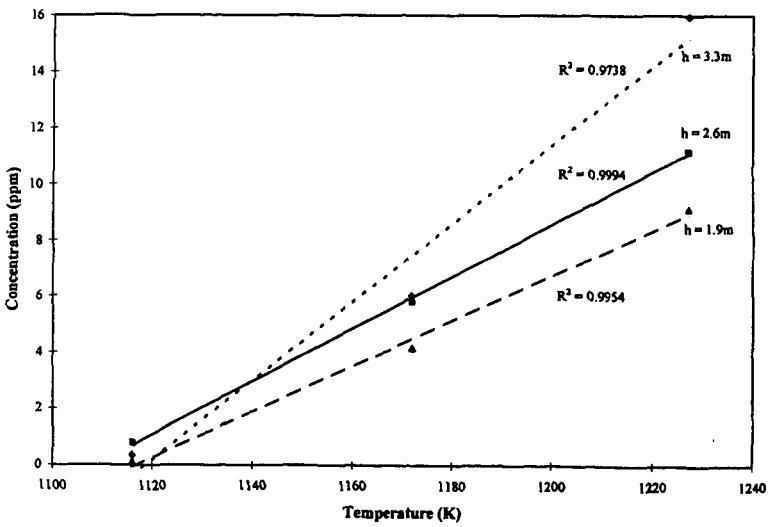

Figure 2. The effect of temperature on the emission of sulfur dioxide at different heights above the fuel injection port.

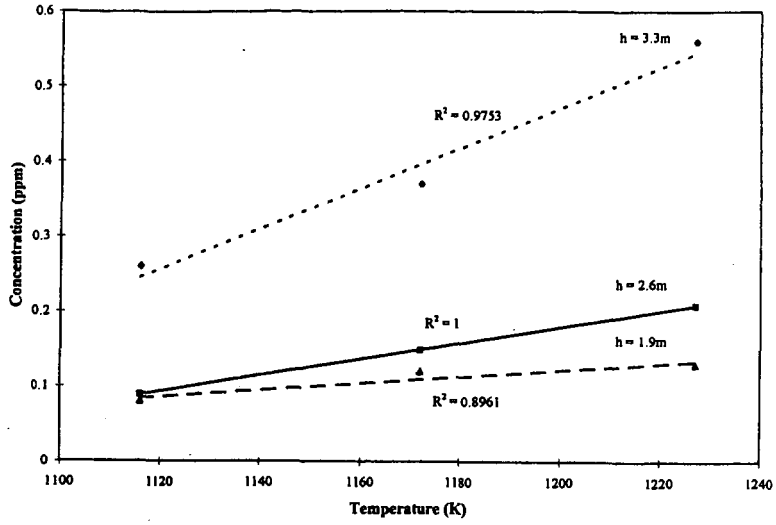

Figure 3. The effect of temperature on the emission of hydrogen chloride at different heights above the fuel injection port.

The Effect of Coal Type. Figure 4 shows the results of sulfur dioxide emission from tests with two different coals (95011 and 95031). It is clear that good sulfur capture is obtained between 1120K and 1170K for both coals. The higher sulfur oxide emission for coal 95011 observed at the higher temperature may be due to the effect of temperature and the higher sulfur content (3%). There is good agreement between the HCl emission and chloride content in the coal, as is illustrated in Figure 5. No chloride containing species were identified in a cold trap solution (methylene chloride with phenol).

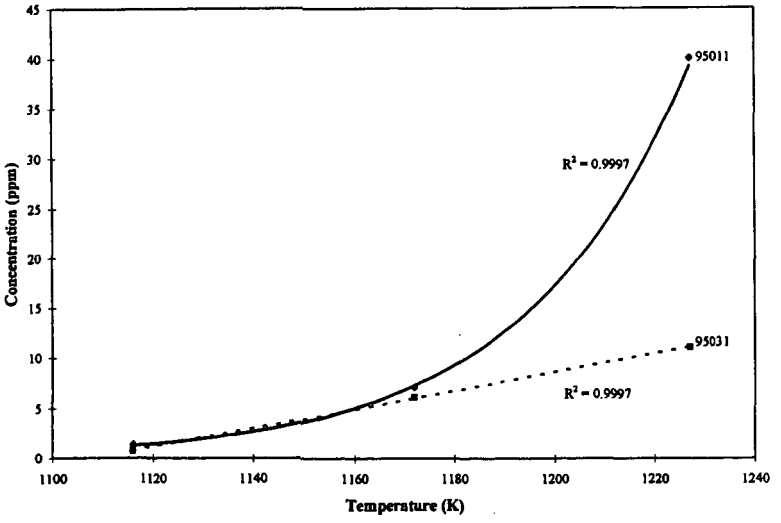

Figure 4. The effect of coal type on the emission of sulfur dioxide at different temperatures in the AFBC system.

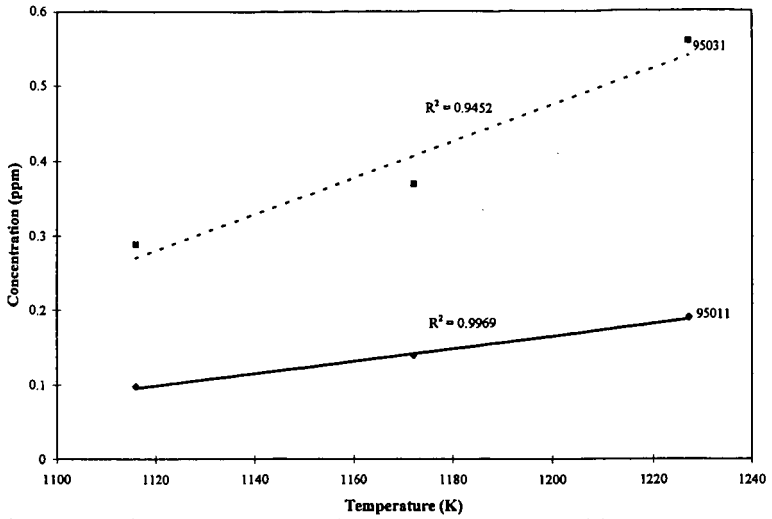

Figure 5. The effect of coal type on the emission of hydrogen chloride at different temperatures in the AFBC system.

The Effect of the Ca/S Ratio. In Figure 6 the measured SO_2 in the flue gas is plotted versus the calcium-to-sulfur molar ratio. The results indicate there is a significant improvement with the sulfur capture with the higher Ca/S ratio in the temperature between 1172 and 1227K. However, there is no effect at the optimal temperature (1116K). In the case of HCl emission, there is no significant difference on the emission of HCl between different Ca/S ratios, as is illustrated in Figure 7.

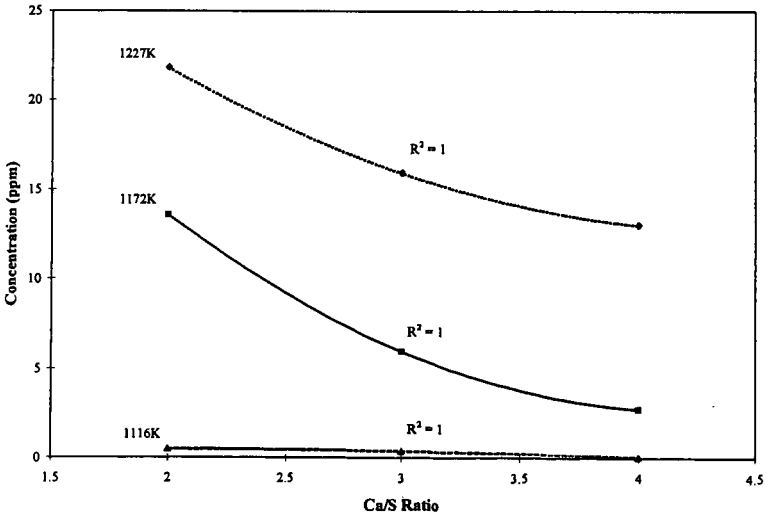

Figure 6. The effect of the Ca/S ratio on the emission of SO_2 different temperatures in the AFBC system.

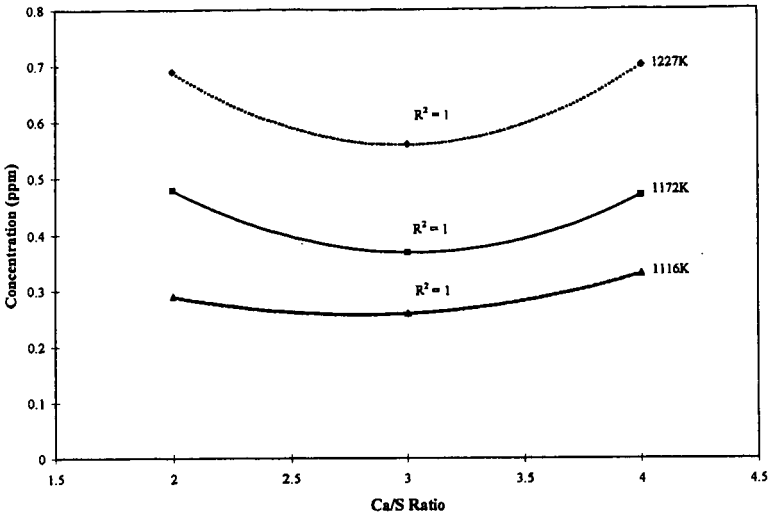

Figure 7. The effect of the Ca/S ratio on the emission of HCl at different temperatures in the AFBC system.

CONCLUSIONS

Based on the information presented in this paper summary statements that can be made include:

- The optimal sulfur retention is obtained around 1120K under our experimental conditions.
- The capture of HCl by limestone is more difficult than the capture of SO_2.
- Molecular chlorine was not identified in any of the flue gases from the AFBC system.
- There is no significant change in the emission of HCl when the Ca/S ratio is varied.

ACKNOWLEDGMENTS

The financial support for this work received from the Electric Power Research Institute is gratefully acknowledged.

REFERENCES

1. Hartman, M.; Hejna, J.; and Beran, Z. *Chemical Engineering Science*, 1979, *34*, 475.
2. Shao, T.; M.S. Thesis, Western Kentucky University, 1994.
3. Heidbrink, Jenny, M.S. Thesis, Western Kentucky University, 1996.
4. Liang, D.T.; Anthony, E.J.; Leowen, B.K.; Yates, D.J. *Proceedings* of the 11th International Conference on FBC, Montreal, Canada, April 21-24, 1991, Volume 2, pp. 917-22.
5. Munzner, H.; Schilling, D.H. *Proceedings* of the 8th International Conference on FBC, Volume III, Houston, March 18-21, 1985, pp. 1219-26.

THE EFFECT OF COAL CHLORINE AND SULFUR CONTENTS ON HIGH TEMPERATURE CORROSION IN AN AFBC SYSTEM

Wei Xie, Shi Su, Brian Sisk, Jeremy Bowles, Wei-Ping Pan and John T. Riley
Materials Characterization Center and Department of Chemistry
Western Kentucky University
Bowling Green, KY, 42101

Keywords: corrosion, combustion, chlorine, sulfur

INTRODUCTION

The occurrence of furnace wall and superheater corrosion in fluidized bed combustor systems has caused some operational and economic concerns.[1] It is generally accepted that chlorine and sulfur may play roles in this corrosion. In order to predict the performance of high chlorine or high sulfur coals in these combustion systems, it is necessary to have a better understanding of the different corrosion mechanisms in which chlorine and sulfur may be involved.[2] It is also important to evaluate the critical point of coal chlorine content which may cause initial corrosion.

TVA's Shawnee plant observed that the boiler tubes in the primary superheater region of the atmospheric fluidized bed combustion system had wastage/corrosion problems between 1992 and 1993. The boiler tubes were located in the bed area and the wastage was caused by both corrosion and erosion. It is difficult to isolate the factors (such as chlorine content, sulfur content, or erosion) causing this wastage. Also, the gas composition varies a great deal in the primary superheater region. However, the tube wastage problems were resolved after several modifications were made in the AFBC system. The modifications included (1) changing the type of coal to a low chlorine coal, and (2) elevation of the boiler tubes to a higher position in the unit.

Our study was designed to evaluate the role coal chloride may play in causing corrosion of boiler components. The Western Kentucky University AFBC system was configured to simulate the Shawnee Plant's system and especially the secondary superheater region in the TVA plant. This simulation excluded consideration of the erosion problems. Also, TVA did not observe any wastage in this location when they used low chloride content coal. The gas composition of this location is very consistent during constant operation.

EXPERIMENTAL

Two 1,000-hour burns were conducted with the 12-inch (0.3 m) laboratory AFBC system at Western Kentucky University. Operating conditions similar to those used at the 160-MW system at the TVA Shawnee Steam Plant located near Paducah, KY were used. A 1000-hour burn was done with a low-chlorine (0.012% Cl and 3.0% S) western Kentucky # 9 coal, which is the same type of coal as that supplied to the TVA plant during 1993. A second 1000-hour burn was conducted with high-chlorine (0.28% Cl and 2.4% S) Illinois # 6 coal. The limestone came from Kentucky Stone in Princeton, KY. This is the source of the limestone used by the Shawnee plant in their AFBC system during 1993. The major operating parameters were as follows: excess air level -- approximately 1.3; Ca/S ratio -- approximately 3; bed temperature -- approximately 1150 K; and temperature near metal coupons -- approximately 900 K. Four different metal alloys [carbon steel C1020 (0.18% C and 0.05% Cr), 304 SS (18.39% Cr and 8.11% Ni), 309 SS (23.28% Cr and 13.41% Ni), and 347 SS (18.03% Cr and 9.79% Ni)] were studied in this project. Each metal coupon had a 5.08 cm outside diameter, was 0.3175 cm thick, with 1.587 cm diameter hole in center. A set of metal coupons was placed at 3.35 m above the fuel injection port, which is 10 cm below the convective pass heat exchange tubes. Coupons were held in place by a machinable tungsten rod (powder metallurgically prepared) and separated by ceramic mounts. Two sets of each coupons (listed above) made a total of eight coupons for the run. Each specimen within a group was rotated as to position in an array every 250 hours during the test burn. The coupon was weighed before and after the run and examined using SEM. The SEM analysis was performed on a JEOL JSM-5400 SEM. Attached to the SEM for Energy Dispersive X-ray analysis (EDS) was a KEVEX Sigma 1 system with a Quantum detector for elemental analysis down to carbon. The following instrument operating parameters were used for the SEM/EDS analysis: electron beam energy -- 20 KeV; working distance -- 24 mm; sample tilt angle -- 0°.

RESULTS AND DISCUSSION

Only SEM/EDS results on different specimens will be presented in this paper. The results of corrosion with respect to the morphologies of the test coupons (cross section examination) will be reported in the near future.

The C1020 specimen was cracked after 250-hours of operation in both test runs. Figure 1 illustrates the weight change data for the alloys in the first 1000-hour burn with the low chloride coal. The type 347 specimen showed the highest weight gain among the other three samples. However, alloy 304 showed the most oxide scale on the surface and alloy 309 showed the least oxide scale on the surface. These observations are based on the color (reddish) and SEM studies. Also, slight scale failures were observed in all three samples. The degree of scale failure is in the following order: 304 > 347 > 309 (the least). This is the reason for the fluctuation of weight change shown for alloy 304. The weight gain is due to the oxidation and the weight loss is due to the scale failure. The two reactions compete with each other.

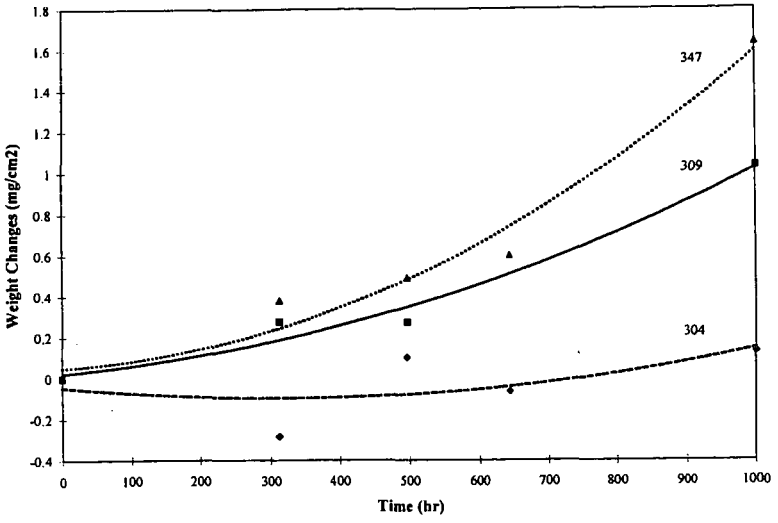

Figure 1. The effect of time of exposure to AFBC combustion gases on the weight of metal coupons.

The scale failure might be due to the sulfur attack and the effect of erosion. The EDS results indicated that the amount of sulfur, calcium and sodium on the surface increased with burning time, as is illustrated in Figures 2 and 3. A certain amount of fly ash passed through the specimens the entire time during the run. Thus, the effect of erosion should also be taken into consideration. The alloy 309 is the best (less oxide scale and scale failure) corrosion resistant material among the three samples under our experimental conditions. It may be due to the high amount of chromium in the compositions.

Figure 4 shows the weight change data for the alloy in the second 1000-hour burn with the higher chlorine coal (0.28% Cl). The weight gain was observed in the case of 309 and 347 before 500 hours. In the case of the 304 alloy, the weight almost remained constant in the first stages of the test burn. There is no chloride (EDS results) observed on the surface of coupons before 500 hours, as is illustrated in Figures 5 and 6. The small amount of scale failure was observed on all three samples, which is similar to the results obtained with the low chlorine coal in the first 1000-hour test. However, the weight loss was observed in all three coupons after 500 hours. The chloride also was identified on the surface of the coupons. Based on the mapping results, the chloride is evenly distributed on the surface of the coupons. There is no concentration of chloride on the spot of scale failure. There are more scale failures observed in this test run than was observed in the first test run. This suggests that chlorine may enhance attack on the metal coupons, but the data is not conclusive.

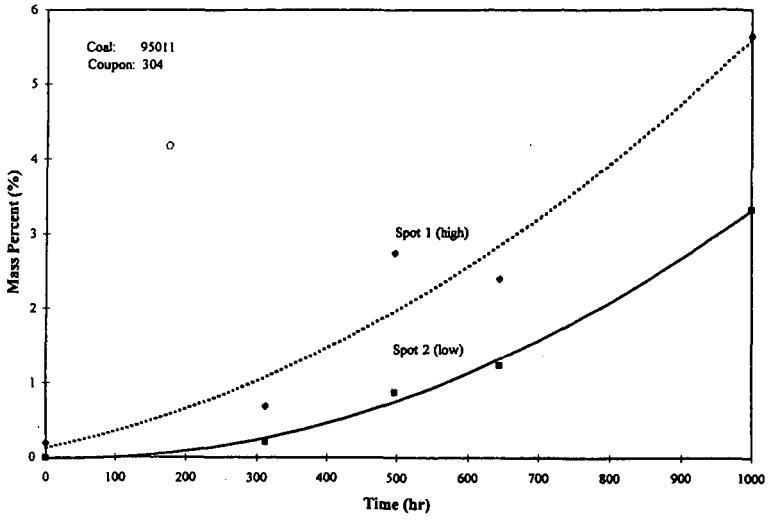

Figure 2. The effect of time of exposure to AFBC combustion gases on the sulfur concentration on metal coupons.

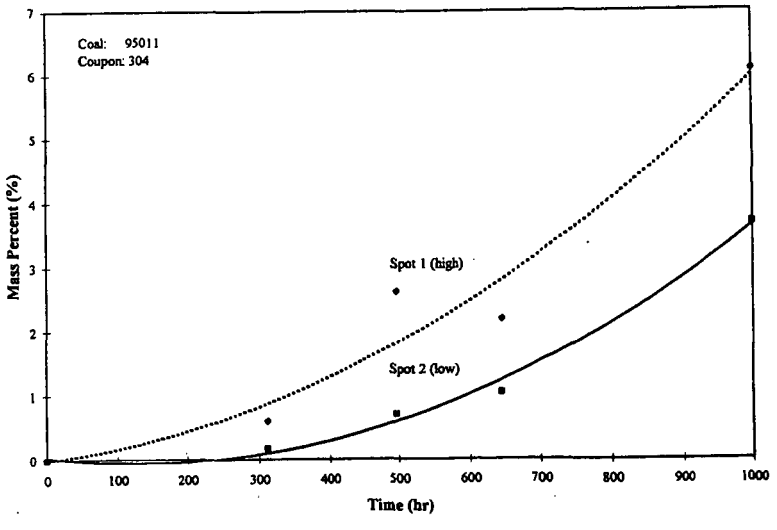

Figure 3. The effect of time of exposure to AFBC combustion gases on the calcium concentration on metal coupons.

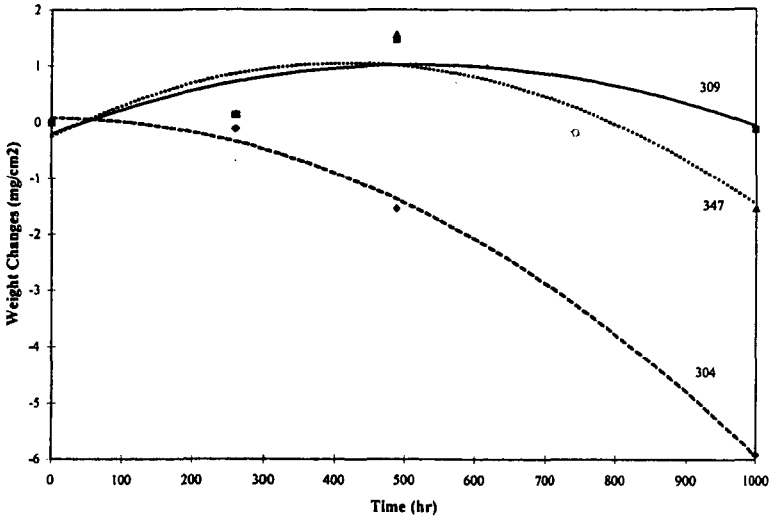

Figure 4. The effect of time of exposure to AFBC combustion gases on the weight changes of metal coupons.

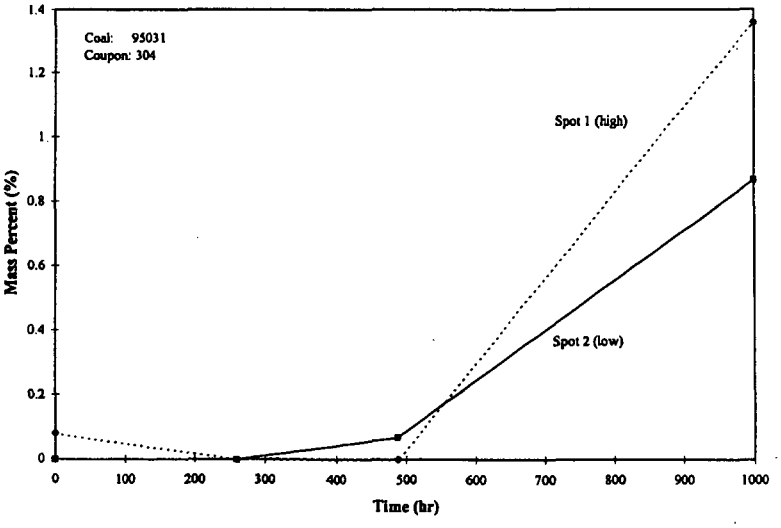

Figure 5. The effect of time of exposure to AFBC combustion gases on the chloride concentration on metal coupons.

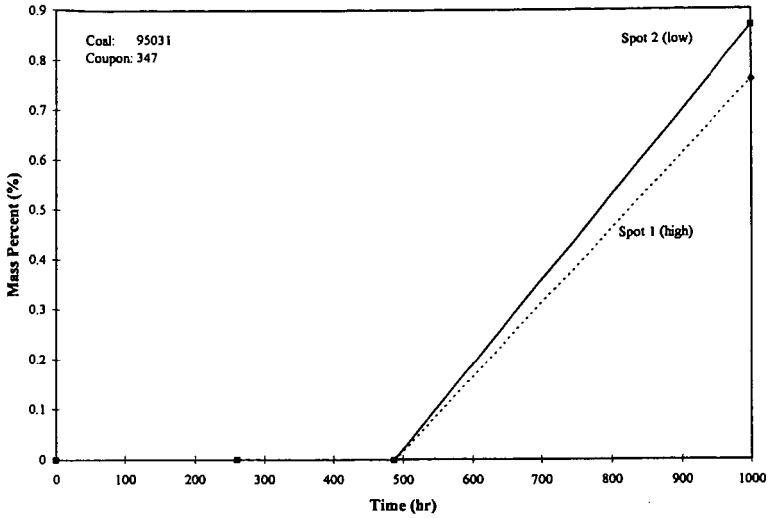

Figure 6. The effect of time of exposure to AFBC combustion gases on the chloride concentration on metal coupons.

CONCLUSIONS

Based on the data presented in this paper the following statements and observations can be made.

- High chromium (~ 23%) 309 alloy steels forming Cr_2O_3 on the surface possessed the greatest corrosion resistance of the four materials tested.
- Scale failure was observed in both 1000-hour test burns with low and high chlorine coals. The second test burn with the high chlorine coal showed more scale failure than that obtained with the first run with the low chlorine coal.
- Chlorine in the coal may enhance the scale failure but the evidence is not conclusive.

ACKNOWLEDGMENTS

The financial support for this work received from the Electric Power Research Institute is gratefully acknowledged.

REFERENCES

1. Minchener, A.J.; Lloyd, D. M.; Stringer J. "The Effect of Process Variables on High Temperature Corrosion in Coal-Fired Fluidized Bed Combustors," in *Corrosion Resistant Materials for Coal Conversion Systems,* (Ed. Meadowcroft, D.B. and Manning, M.I.) Chap. 15, Applied Science Publishers, New York, 1983, p. 299.
2. Mayer, P.; Manolescu, A.V.; Thorpe, S.J. "Influence of Hydrogen Chloride on Corrosion and Corrosion-Enhanced Cracking Susceptibility of Boiler Construction Steels in Synthetic Flue Gas at Elevated Temperature," in *Corrosion Resistant Materials for Coal Conversion Systems,* (Ed. Meadowcroft, D.B. and Manning, M.I.) Chap 5, Applied Science Publishers, New York, 1983, p. 87.